Risk Based Dynamic Security Assessment

by

Anuradha Dissanayaka

A Thesis submitted to the Faculty of Graduate Studies in partial

fulfillment of the requirements for the Degree of

Master of Science

The Department of Electrical and Computer Engineering

The University of Manitoba

Winnipeg, Manitoba, Canada

UNIVERSITY OF MANITOBA | Faculty of Graduate Studies

Master's Thesis/Practicum Final Report

The undersigned certify that they have read the Master's Thesis / Practicum entitled:

Risk Based Dynamic Security Assessment

Submitted by

Anuradha Dissanayaka Mudiyanselage

The Thesis / Practicum Examining Committee certifies that the thesis / practicum (and oral examination is require) is:

APPROVED

(Approved or Not Approved)

☒ Thesis ☐ Practicum

Name/Unit:	Signature
Dr. U. Annakkage, ECE Advisor	[redacted]
CoAdvisor	
CoAdvisor	[redacted]
Dr. A. Gole, ECE	
Dr. P. Thulasiraman, CS	[redacted]

Date: AUG 16 2010

To my wife and son.

Acknowledgements

First of all, I would like to express my sincere gratitude to my advisor, Professor Udaya Annakkage for his continuous advice, guidance and encouragement throughout the course of this work. I consider myself privileged to have the opportunity to work under his guidance. I greatly appreciate the advice and assistance received from Dr. Bathiya Jayasekara with the transient stability polynomial. I am also grateful to Dr. Bagen Bagen of Manitoba Hydro for useful inputs received during valuable discussions.

The financial support received from the Manitoba Hydro and the provincial government of Manitoba in the form of Graduate Scholarship is greatly appreciated.

I would like to thank all my friends and the staff of the Department of Electrical and Computer Engineering for their continuous encouragement and for making my years at the University of Manitoba a pleasant experience.

This acknowledgement would not be complete without thanking my family. I extend my heartfelt gratitude to my wife and son. They were always understanding and encouraging me during my hard times. I would also like to thank my mother and sister for all the love and support.

Anuradha Dissanayaka

August 2010

Abstract

This thesis presents a linearized technique to determine a risk-based index for dynamic security. The method is an extension to an existing technique in which the risk of steady state security is calculated using the mean and variance of load uncertainty. The proposed method is applied to calculate the risk indices for the New England 39 bus test system. The results obtained from the proposed method are validated against those estimated by Monte Carlo simulation. Both approaches produce virtually the same results for small load deviations

Table of Contents

1 Introduction 1
  1.1 Overview . . . 1
  1.2 Power System Reliability . . . 2
  1.3 Power System Security . . . 3
  1.4 Power System Security States . . . 6
  1.5 Concept of Risk . . . 8
  1.6 Thesis Objectives . . . 9
  1.7 Thesis Outline . . . 11

2 Deterministic and Probabilistic Security Assessment 13
  2.1 Introduction . . . 13
  2.2 Security Assessment . . . 14
    2.2.1 Deterministic Approach . . . 14
    2.2.2 Probabilistic Approach . . . 16
    2.2.3 Comparison of the Probabilistic and Deterministic Approaches 19
  2.3 Dynamic Security Assessment . . . 22
  2.4 Risk Based Security Assessment . . . 23
    2.4.1 Risk . . . 23
    2.4.2 Severity . . . 28
    2.4.3 Uncertainty of operating condition . . . 29
  2.5 Concluding Remarks . . . 31

3 Risk Based Static Security Assessment 32
  3.1 Introduction . . . 32
  3.2 Newton Raphson Power Flow . . . 33
    3.2.1 Power Flow . . . 34
    3.2.2 Line Flow . . . 38
  3.3 Risk Based Voltage Security Assessment - Linearized Method . . . 40
    3.3.1 Uncertainty of Operating Condition . . . 41
    3.3.2 Uncertainty of Contingency . . . 44
    3.3.3 Severity . . . 46
    3.3.4 Risk Calculation Procedure . . . 49
  3.4 Risk Based Overload Security Assessment - Linearized Method . . . 53
  3.5 Validation against the Non-Linear model using Monte Carlo Simulation 59
    3.5.1 Comparison of Linear and Non Linear results . . . 60
  3.6 Concluding Remarks . . . 62

4 Risk Based Dynamic Security Assessment 64
4.1 Introduction 64
4.2 Transient Stability Margin in Functional form 65
4.3 Probability Distribution of Stability Margin 67
4.3.1 Linear Method 67
4.3.2 Non Liner Model using Monte Carlo Technique 72
4.3.3 Comparison of Probability Distributions 75
4.3.4 Risk Calculation 77
4.4 Concluding Remarks 80

5 Applications and Issues 81
5.1 Introduction 81
5.2 Applications and Issues with One-Hour-Ahead Forecast 81
5.3 Applications at the Control Room 82

6 Conclusions 84
6.1 General Conclusions 84
6.2 Contributions 86
6.3 Suggestions for Future Research 86

Appendices

A Test Systems Data 88
A.1 New England 39 Bus System 88
A.1.1 Single Line Diagram 88
A.1.2 Power Flow - AC Bus Data 89
A.1.3 Power Flow - Load Data 90
A.1.4 Power Flow - Generator Data 90
A.1.5 Power Flow - Line Data 91
A.1.6 Dynamic Data - Generators 92
A.1.7 Dynamic Data - Exciters (IEEET1) 92
A.1.8 Dynamic Data - Stabilizer (STAB1) 92

Acronyms 93

Reference 98

List of Figures

1.1 Power System Security Classification 4
1.2 Power System Operating States 7

2.1 Risk based security assessment calculation. 26
2.2 Continuous severity function 29

3.1 Typical bus of the power system. 34
3.2 Simple Transmission line model 39
3.3 Poisson distribution for different λ 45
3.4 Severity Function for low voltage 48
3.5 Severity Function for over load 48
3.6 Continuous severity function for transient stability margin 50
3.7 Risk Calculation 51
3.8 Voltage Risk Indices for Contingency 01. 52
3.9 Voltage Risk Indices for Contingency 02. 53
3.10 Line Flow Risk Indices for Contingency 01. 57
3.11 Line Flow Risk Indices for Contingency 02. 57
3.12 Voltage Risk from Non-Linear and Linear methods for contingency 01. 61
3.13 Voltage Risk from Non-linear and Linear methods contingency 02. . . 61

4.1 Flowchart of Linear approximation method. 71
4.2 Histogram and equivalent normal distribution of Transient Stability Margin for 10,000 cases with 2% load standard deviation for contingency 1. 73
4.3 Flowchart of Monte Carlo based simulation. 74
4.4 Histogram and equivalent normal distribution of Transient Stability Margin for 10,000 cases with 10% load standard deviation for contingency 2. 75
4.5 Percentage error of mean and standard deviation with load standard deviation for contingency 01. 76
4.6 Percentage error of mean and standard deviation with load standard deviation for contingency 02. 76
4.7 Continuous severity function for transient stability margin. 77
4.8 Risk comparison for contingency 01. 79
4.9 Risk comparison for contingency 02. 79

A.1 Single Line Diagram of IEEE New England 39 Bus System. 88

List of Tables

1.1 Data of an accidents 9

2.1 Risk values for two Accidents for different operating conditions . . . 24
2.2 Total Risk for the glass factory with two different machines with two accidents 25

3.1 Voltage Risk for Contingency 1 and 2 52
3.2 Line Flow Risk Indices for Contingency 1 and 2. 58
3.3 Voltage risk from Non-linear and Linear methods for contingency 01. 62
3.4 Voltage risk from Non-linear and Linear methods for contingency 02. 63

4.1 Mean, standard deviation and percentage error of Stability Margin by Non Linear and Linear methods for contingency 01. 75
4.2 Mean, standard deviation and percentage error of Stability Margin by Non Linear and Linear methods for contingency 02. 76
4.3 Risk values for two contingencies for different load standard deviation levels. 78

Chapter 1

Introduction

1.1 Overview

The liberation of the electricity market and the increasing utilization of renewable generation for electric power supply introduced many uncertainties in electric power systems. This often results in highly stressed system conditions, and system operators are frequently forced to operate power systems with small stability margins under uncertain operating conditions. Planning and operating bulk interconnected power systems are complex activities that require involvement of large number of people bridging a wide range of experiences and interests. In the early days this was the domain of the planning and operating engineers who attached to the utility company. However, now there are people representing various interests and needs, which includes of transmission owners, system operators, energy sellers, large industrial customers and other end users, regulators, reliability councils, security centers, manufactures, marketers, brokers and power exchange personal.

As a result of these different categories of participants, the operating conditions of the power system become more stressed. Furthermore, the loading pattern of the transmission system differ from those for which they were originally designed. As a result of current technical advancements, the controllability and observability of the power system have been improving. The controllability is achieved due to the installation of advanced control systems. The availability of high tech monitoring and communication systems generate large amount of data about the power systems. Therefore, this further increases the complexities of the power system.

As a result of market oriented thinking and stressed operating conditions, there is a significant deterioration of reliability level which develops social and economic impact. This directly counter benefits the decrease of energy costs brought by market competition. Therefore, to keep proper planning and operation of power systems, maintaining the reliability of the power systems is prime importance tasks.

1.2 Power System Reliability

The reliability of the power system is defined by North American Reliability Council ($NERC$) as "Reliability in a bulk power electric system, is the degree to which the performance of the elements of that system results in power being delivered to consumers with accepted standards and in the amount desired. The degree of reliability may be measured by the frequency, duration and magnitude of adverse effects on the consumer service". The reliability can be addressed by considering two basic functional aspects of the power system called adequacy and security. The adequacy of the power system is defined as the ability of the power system to supply the aggregate electric power and energy requirements of the customers at all times, by taking into account the scheduled and unscheduled outage of the system components. The security of the power system is defined as the ability of the power system to withstand sudden disturbances such as electric short circuits or non anticipated loss of system components [1, 2]. The main intention of this thesis is to analyze the power system security by considering the probabilistic nature of operating conditions.

The power system disturbances can occur at any given time and this may lead to line overload, voltage violation/collapse and transient instability. As a result of these disturbances, protection relays may operate and this may lead to uncontrollable cascading conditions. According to power system reliability definitions, power should be delivered with acceptable quality and in required quantity. To supply continuous uninterrupted power, risky operating conditions have to be identified and necessary steps should be taken to minimize the risk. The reliability studies are normally carried out to identify the severity of the disturbances and to keep the power system reliability at adequate levels.

1.3 Power System Security

Security of a power system refers to the degree of risk in its ability to survive imminent disturbances without interruption of the customer service. Therefore, it is a measure of robustness of the system to withstand sudden disturbances. Hence, power system security depends on the system operating condition as well as the contingent probability of disturbances [3].

The security assessment is performed to ensure the security of the power system, and it can be categorized as static security assessment and dynamic security assessment. The static security assessment determines whether the steady state post disturbance conditions violate any device limits or voltage limits. That assures whether the power system reaches an acceptable operating condition after the transition. The dynamic security assessment determines whether the power system reaches a new equilibrium operating point or not after the transition.

The static security assessment can be used to quickly determine whether the system is insecure by simply looking at the static outcome of the contingency. However, to know whether the system is fully secured, dynamic security assessment must be performed.

As shown in Figure 1.1, power system security can be classified into different categories based on the static and dynamic nature of the problem.

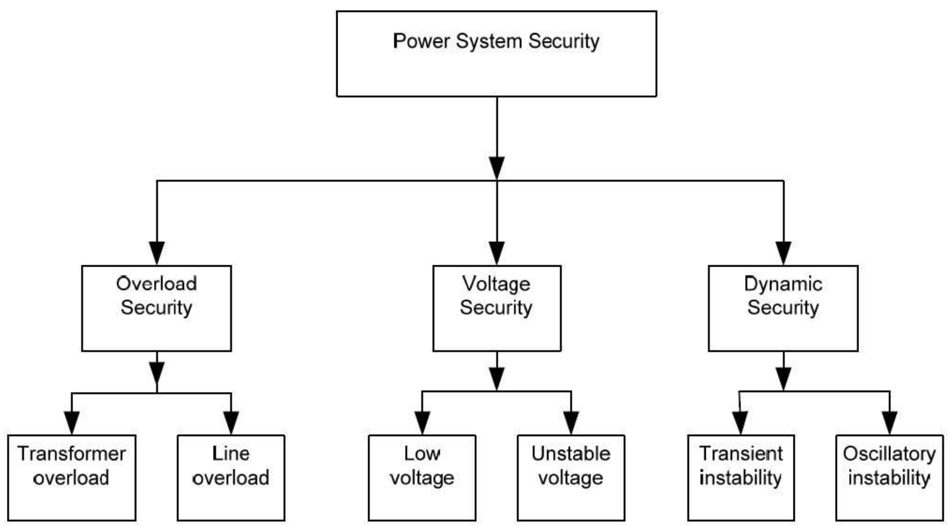

Figure 1.1: Power System Security Classification

Initially, it is categorized into three sections, namely overload, voltage and dynamic security. The overload security can be divided into transformer overload and line overload security. The voltage security can be divided into low voltage security and unstable voltage security. The low voltage security assess whether voltages of the power system decrease below the devise ratings. The unstable voltage security examines behavior of the voltage with system load levels as well as voltage collapse with system load levels. Both overload and low voltage security describe the violation of device limits, and therefore can be categorized as static security. Both line overload and low voltage security are discussed in Chapter 3 under static security assessment. The analysis of unstable voltage has been done in both static and dynamic ways in the literature [4, 5]. Therefore, unstable voltage security can be categorized as static or dynamic security. The dynamic security can be categorized into transient instability and oscillatory instability. In Chapter 4, transient stability security is discussed under dynamic security assessment.

Both static and dynamic security assessment can be carried out in deterministic or probabilistic manner. The deterministic security assessment introduces power system operation limits based on the impact of contingencies. In the probabilistic approach, these operating limits are calculated by considering both impact and probability.

Currently, deterministic techniques are widely used to assess the security of power systems. In a deterministic approach, a set of contingencies is identified and power system is designed to operate reliably when these contingencies occur. In practical applications, this is considered as loss of any single component of the power system such as a generator, a transformer or a transmission line. This is usually refereed to as N-1 approach as this method studies the behavior of the N element power system after the loss of any one of its elements [3]. Deterministic security assessment techniques have been used for several decades to check the reliability of the power system and generally it leads to build up highly secured strong power systems. Apart from the high cost due to conservative designs, the main drawback with a deterministic assessment technique is that, it treats all security problems to have equal risk [3]. In a deterministic approach the contingencies are selected based on the probability. Therefore, to some extent the probability of events is considered. However, once the contingencies are selected they are treated as equally probable. Also, it does not take into account the probability of operating conditions. In a deterministic approach, there is no economical evaluation technique available to analyze the security level of the power system and therefore, may not be possible to make economical decisions in the control room environment by ensuring the security.

1.4 Power System Security States

The power system security states represents different types of operating conditions, which gives an indication about the security of the power system. The classification of power system states are very important to build the foundation of the power system security analysis. This analysis can be used to select appropriate control systems and to keep the system secure during disturbances. In the literature, power system states are classified into five different states namely *normal, alert, emergency, in extremis and restorative* [6, 7]. Figure 2.1 shows these operating states and the ways in which transition can take place from one state to another.

The operation of the power system can be described using three sets of generic equations: one differential and two algebraic equations. The differential equations encode the physical laws governing the dynamic behavior of the system's components. The two algebraic equations consist of equality constraints (E), which refers to the systems total load and total generation and inequality constraints (I), which refers to the system variables, such as currents and voltages.

In *normal state*, all system variables are within the normal range of operation, and no equipment is being overloaded. The system operates in a secure manner and is able to withstand a contingency without violating any of the constraints.

The system enters into the *alert* state if the security level falls below a certain limit of adequacy. In this state, all system variables are still within the acceptable range and all constraints are satisfied. However, the system has been weakened to a level,

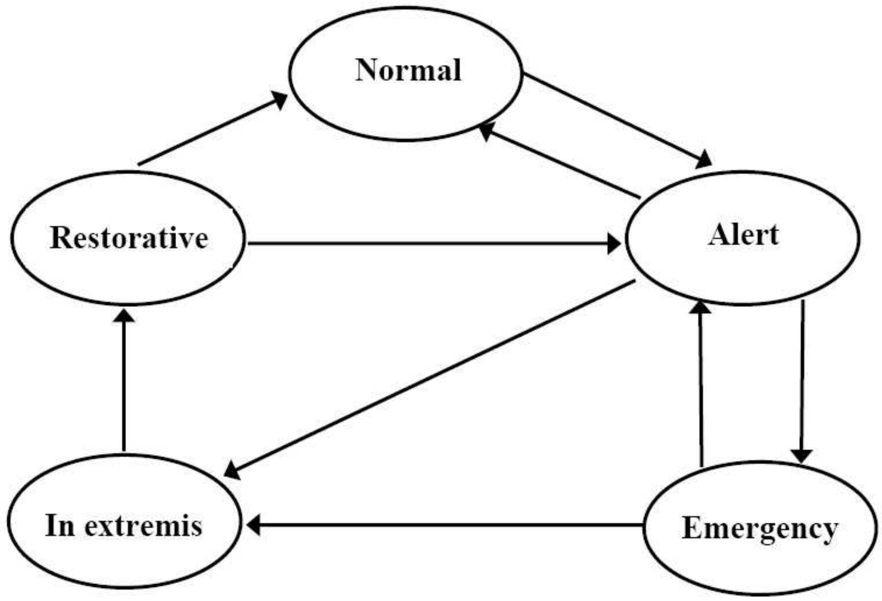

Figure 1.2: Power System Operating States

where a contingency may cause an overloading of equipment by violating inequality constraints that places the system in an *emergency state*. If the disturbance is very severe, the state may change to the *in extremis state* from the *alert state*.

Preventive actions, such as generation shifting or increased reserve can be taken to restore the system to *normal state*. If the restorative steps do not succeed, the system remain in the *alert state*.

When sufficiently severe disturbance occurs during the *alert state* the system enters into *emergency state*. In this state, inequality constraints are violated. However, the system is still intact and may be restored to the *alert state* by initiating emergency control actions such as fault clearing, excitation control, fast-valving, generation tripping, generation run-back, HVDC modulation, and load curtailment etc.

If the above measures are not taken or are ineffective, the system is *in extremis state* and the result is cascading outages and possibly a shut down of a major part of the system. If system reaches to this stage then both system equality and inequality constraints are violated. To prevent this kind of situation, emergency control actions, such as load shedding and controlled system separation can be done to save the system as much as possible from a widespread blackout.

If control actions are successful then the system goes to *restorative state*. In this state further control actions are taken to reconnect all the facilities and to restore the system load. Finally, the system transfers from this state either to the *alert state* or to the *normal state* depending on the system conditions.

The objective of the security assessment is to identify the possible threat to the power system and take preventive control actions to ensure *normal state* operating conditions. Therefore, security assessment basically deals with *normal* and *alert states*.

1.5 Concept of Risk

In this thesis, security of the power system is analyzed by considering the risk of different operating conditions with different contingencies. The risk is the systems exposure to failure, and it is obtained by considering both the probability of occurrence of an event and the impact of the event. However, general usage of risk tends focus only on potential harm that may arise from a future event, which may accrue either from incurring a cost or by failing to attain some benefit. In mathematical terms risk can be defined as in Equation 1.1.

$$Risk = (Probability\ of\ event\ occuring) \times (Impact\ of\ event\ occuring) \qquad (1.1)$$

Table 1.1: Data of an accidents

Event	Probability	Impact
Accident I	0.05	20
Accident II	0.02	25

To identify the concept, consider the example given in Table 1.1 related to a glass factory. The probability is the occurring probability of an accident and impact is the number of damaged glass bottles due to that accident. Therefore, according to Equation (1.1) risk of the Accident I is 1.0 and Accident II is 0.5. Accident I is more risky than accident II as the occurring probability is high even though it damages less bottles than Accident II. In general, it might be thought that Accident II is severe due to high impact. However, it is not the correct approach. In pure deterministic approach, Accident II should be prevented first. However, in probabilistic approach Accident I is the most destructive one, and it should be prevented first.

1.6 Thesis Objectives

The main objective of this research is to develop probabilistic dynamic security assessment techniques to analyze the security of the power system. The main goals were identified and work is carried out to reach the objectives. During the development stages of the risk based or probabilistic dynamic security model, the followings were achieved in order to reach the main objective of this research.

1. Investigation of exiting probabilistic security assessment techniques which is commonly known as risk based security assessment. The model developed in [8] is analyzed by calculating static security index for low voltage and line overloads. This investigation revealed that risk indices can be calculated using normally distributed P and Q load model. Furthermore, this load model with linear approximated techniques can be used to develop new techniques to calculate risk based dynamic security index with less amount of computing power as well as within short period of time.

2. Development of theoretical basis to obtain the risk based dynamic security index. The different type of sensitivities are obtained from power flow Jacobian matrix and functional form of transient stability boundary presented in [9].

3. Development of the linear approximated method to do risk based dynamic security assessment by using the polynomial of transient stability boundary generated from machine learning techniques in [9] which have been used to obtain the transient stability boundary. As this polynomial is differentiable with respect to V and δ, required sensitivities are calculated to obtain the probability distribution of the transient stability margin.

4. Development of data generation software model required to carry out the Monte Carlo simulation to check the accuracy of the linear approximated risk based security assessment model.

5. Validation of developed risk based dynamic security assessment model by employing Monte Carlo simulation. The data generation software model is used to check the accuracy of probability distribution of stability margin as well as risk indices.

6. Development of MATLAB codes for data generation model, risk based low voltage security assessment model, risk based over load security assessment model and risk based transient stability margin security assessment model.

1.7 Thesis Outline

The **Chapter 2** presents the different type of security assessment techniques used in the past. The procedure for deterministic security assessment is described from the beginning. The need of probabilistic security assessment is emphasized for new power system environment. A brief comparisons is given between deterministic and probabilistic security assessment. The possible ways of overcoming the problems with traditional deterministic approach is discussed. The risk based dynamic security assessment is introduced.

The risk based static security assessment of the power system is presented in **Chapter 3**. The Newton Raphson power flow is developed and the Jacobian matrix is obtained to get the required sensitivities to find the probability distribution of bus voltages. The power system line flow equations are also developed and the first order partial derivatives of line flows are derived by differentiating the line flow equations with respect to V and δ. The partial derivatives are used to find the probability distribution of the line flow. The risk based static security index is calculated for low voltage and line flow using obtained probability distribution and continuous severity function. The risk indices are validated using Monte Carlo simulation.

The risk based dynamic security assessment is carried out in **Chapter 4**. The functional form of the transient stability margin is used to find the critical clearing time for a particular contingency. As this polynomial is differentiable, necessary sensitivities are calculated by differentiating with respect to V and δ. The Jacobian matrix obtained in Chapter 3 is used to get partial derivatives of load P and Q with respect to V and δ. By using these two types of sensitivities partial derivatives of stability margin with respect to load P and Q are calculated. The probability distribution of the transient stability boundary is calculated using linear techniques. The risk index is obtained using probability distribution of transient stability boundary and continuous severity function. The Monte Carlo simulation is used to validate the accuracy of the linear approximated method.

The applications and issues of the proposed risk bases dynamic security index have been presented in **Chapter 5**.

The conclusions of the research is presented in **Chapter 6** and recommended future studies are also discussed.

Chapter 2

Deterministic and Probabilistic Security Assessment

2.1 Introduction

In the deterministic approach the contingencies are selected based on the probability. Therefore, to some extent the probability of events is considered. However, once the contingencies are selected they are treated as equally probable and operation limits are introduced based on the impact of contingencies. In the probabilistic approach, these operating limits are calculated by considering both impact and probability.

To develop a reliable security assessment tool, the shortcomings of the existing deterministic techniques should be identified. For that, the procedure of existing deterministic method is discussed with a comparison of the procedure of probabilistic security assessment. Some of the identified prevailing problems of the traditional deterministic method are corrected by employing the probabilistic approach. The risk based approach is selected as the basis for the probabilistic dynamic security assessment, and the theory developed in literature is presented with necessary formulas. A brief description of dynamic security assessment is introduced and the importance of studying dynamic behavior of the power system with complex dynamic components are emphasized.

Security assessment has become complex with the introduction of advanced power system control systems. The situation get aggravated with the unpredictable nature of the power system. Therefore, risk based security assessment is a good solution to analyze complex power systems.

2.2 Security Assessment

2.2.1 Deterministic Approach

The reliability studies are carried out to identify the severity of the disturbances and to keep the power system reliability at adequate levels. Currently, the deterministic security assessment techniques are used to assess the security of power systems. In the deterministic approach, contingency set is identified and power system is designed to operate reliably with these selected contingencies. In the practical environment, this is considered as loss of any single component of the power system such as a generator, a transformer or a transmission line. This is usually refereed to as *N-1* approach, because this method studies the behavior of the N element power system after the loss of anyone of its elements. The deterministic approach proposes a strong power system and operate with large a security margin even though investment and operational cost are high. This has resulted in corresponding high reliability levels in most power systems [10]. The deterministic security assessment is performed in six basic steps when constructing a deterministic security boundary [11]. These steps are,

I. Develop power flow base cases corresponding to the time period (year, season) and loading conditions (peak, partial peak, off peak). In each base case, the unit commitment and network topology are selected based on the expected condition for the chosen time period. The selected topologies normally have all circuits in service. In addition, short term operational studies are often performed with the explicit purpose of identifying the limits for topologies expected in the near future.

II. Select the contingency set. Normally, this set consists of credible events for which post contingency performance could be significantly affected by the study parameters. In deterministic studies, the "*N-1*" rule is used where events are limited to only those involving loss of one component.

III. Identify the study parameters and their ranges of operating conditions expected during the time period of interest. These study parameters are typically, the generation levels for specific generators and the power transfer over specific transmission paths.

IV. Identify the event or events that "first" violate the performance evaluation criteria as operational stress is increased within the study range. These events are referred to as limiting contingencies. If there are no such violations within the study range, the region is not security constrained, and the study is complete.

V. Identify the set of operating conditions within the study range where a limiting contingency "first" violate the performance evaluation criteria. This set of operating conditions defines: a line that partitions study range when we consider two study parameters, a surface when there are three study parameters or a hyper surface for more than three study parameters. This line, surface or hyper surface is the security boundary.

VI. Condense the security boundary into a set of plots or tables that can be easily understood and used by the operator. Nomograms are one of the common ways of expressing the security boundaries.

2.2.2 Probabilistic Approach

Deterministic security assessment techniques have been used for several decades to check the reliability of power systems and generally it leads to build up highly secured strong power systems. Apart from the high cost due to conservative designs, the main drawback with a deterministic assessment technique is that it treats all security problems to have equal risk [3]. In a deterministic approach, the contingencies are selected based on the probability. Therefore, to some extent the probability of events is considered. However, once the contingencies are selected, they are treated as equally probable. Also, it does not take into account the probability of operating conditions. In a deterministic approach, there is no economical evaluation technique available to analyze the security level of the power system and therefore, may not be possible to make economical decisions in the control room environment by ensuring the security. However, the risk based or probabilistic approach can be used to enhance the security-economy decision making at the control room environment [8]. This is achieved by reflecting the accurate power system risk levels and taking the decisions based on it.

In today's competitive market environment, different participants try to maximize their profit and therefore, the power demand and supply experience unexpected variations. Existing deterministic approaches are not adequate to analyze the security of the power system with uncertain market environment and increased uncertainties. In existing traditional power systems like Manitoba, much of the interest is currently diverted to renewable sectors like wind power and solar power. Naturally, availability of renewable generators are highly uncertain and depend on the current weather conditions. Therefore, deterministic security assessment approaches can not be used effectively. Furthermore, deterministic methods normally set up large security margin to operate. Consequently, available facilities may not be fully utilized. This could lead to high operational cost and more investment may be required to keep the higher operating margins. This is not acceptable in any kind of power system environments such as traditional or liberalized. In order to get the maximum output from existing facilities and efficiently use the available resources, power system should operate with acceptable minimum safety margins. The acceptable safety margins should be accurate to avoid possible system collapse as misrepresentation might lead system failures. The deterministic safety margins do not give accurate representation of system risk. Therefore, probabilistic nature of operating conditions and contingencies should be included in the security assessment. Risk based approach incorporates probability of operating conditions and contingencies and presents system risk at a given moment. A comprehensive comparison between deterministic and probabilistic approach is given in [10, 11]. The advantages of probabilistic approach against deterministic approach is widely emphasized in the above comparisons.

Considerable effort has been devoted to power system security assessment using probabilistic techniques. Basic concepts of probabilistic dynamic security assessment have been introduced in early 1980s [12, 13, 14]. The probability of stability indices have been developed by incorporating probabilistic aspects of type, location and clearance of the system faults. In mid 1990s transient stability indices have been introduced based on the stochastic modeling of high speed reclosing [15] and reduced the computation time of the stochastic evaluation using the bisection method [16].

The same authors developed a probabilistic conceptual framework to evaluate the health of the composite generation and the transmission systems [17]. The health of the power system was assessed by incorporating steady state, voltage and transient stability of the power system.

In another approach, the probabilistic transient stability assessment has been done using Monte Carlo type simulation by developing stochastic models of fault type, fault location and load level from historical data and compared with the traditional deterministic results in [18, 19]. Most of the previous works considered stochastic modeling of power system uncertainty to study the affect on transient stability.

The risk based approach has been successfully used in many fields such as nuclear power and money market to asses the security with uncertain environment conditions. The risk based static security indices have been introduced in [8, 20, 21] using linearized analytical approach. Risk indices have been calculated for low voltage, line overload and voltage stability with uncertain loading conditions. The calculated risk indices are based on the predefined set of contingencies and their probabilities of occurrence. The effect of uncertainty of loading conditions are considered and assumed that it is normally distributed around its expected values.

The most of the previous work in probabilistic dynamic security assessment are not simple, and stochastic modeling is time consuming as thousands of simulations are required to model the probability distribution. These time consuming methods are not suitable for one-hour-ahead control room decision making. However, linearized analytical risk based approach of static security assessment is simple and quick. Also, it can be used to assess much larger power systems within short period of time. In [9] the transient stability margin has been derived as a polynomial expressed in terms of voltage magnitudes and phase angles. This enables the extension of the method proposed in [8, 20, 21] to dynamic security analysis. This thesis demonstrates how the method is extended, and then the results are validated against Monte Carlo simulation.

In probabilistic security assessment steps I to III and VI remain as in Section 2.2.1. However, steps IV and V have to be modified as follows [11].

IV. Evaluate the probabilistic indices throughout the study range. Decide on a particular threshold level beyond which operation is deemed unacceptable.

V. Identify the set of operating conditions within the study range that have an index equal to the threshold level. This set of operating conditions constitutes the line (for two study parameters), a surface (for three) or hyper surface (for more than three) that partition the study range. This line, surface or hyper surface represented the security boundary. This boundary identifies the acceptable regions of operation.

In this thesis, risk based dynamic security indices are calculated for voltage, line flow and transient stability margin. The risk based indices are used to identify whether system is secure or not. In probabilistic approach, step V results in a contour or surface of constant risk. In step VI deterministic security boundary is replaced by the iso-risk boundary.

2.2.3 Comparison of the Probabilistic and Deterministic Approaches

The probabilistic approaches are widely used in various decision making environments such as nuclear power, finance, process control and aerospace industries when the outcome is associated with uncertainties.

The deterministic approach is a much simple transparent method and it serves the power industry very well. Therefore, acceptance for probabilistic approach is slow mainly because it is still acquiring the level of credibility as the deterministic approach.

The drawbacks of deterministic approach can be identified as follows [10]:

1. Existing facilities are not fully utilized and system become overbuild.

2. It is difficult to economically evaluate the security level. Therefore, it is difficult to integrate security into economic decision making.

3. The occurrence frequency of events is not measured. For some problems such as overload and voltage security, measures of event severity do exist, e.g., over current or under voltage, and these measures are used within deterministic assessment to judge security level. Yet the measures do not account for events occurrence frequency. Application of the deterministic approach accepts the implicit assumption that all the events in the contingency set occur with equal frequency. However, in power systems, significant variation in occurrence frequency may exist.

4. It ignores the effects of uncertainty in operating conditions.

5. The deterministic approach is unable to recognize the composite influence of more than one contingency. As a result, operation decisions are made that address only the effect of contingencies with highest impact to the power system.

The deterministic approach limits the contingency set to "*N-1*" contingency approach. It uses simple, traditional performance requirements and decisions are taken for the worst case. These security assessment methods were acceptable under the early industry structures as frequency of stressed operating conditions were minimal. Therefore, simple methods were used as a result of difficulties in assessing the uncertainties with high amount of computation requirements.

The security contours can be drawn with power system operating parameters such as V and δ. The method used to draw security boundary in Section 2.2.1 can be used to draw security contours. This contours have equal security levels. The security contours generated from deterministic security assessment does not necessarily results in constant risk [22]. Therefore, decisions associated with deterministic security assessment may results in either very low risk or unintended high risk. This is the problem that is directly answered by risk based security assessment.

But today, all the power system operators want to fully utilize the exciting facilities such as generators and transmission lines and get maximum return on investment. Even though deterministic approach suggested strong overbuild system, it also reduces the profit margin due to transmission constraints. The transmission constraints presented by deterministic approach unnecessarily limits the power flow through transmission lines as deterministic approach considers the worst case scenario. The power system owners do not prefer these situations. On the other hand, computational speed has dramatically increased, and fast computers are available that can effectively be used to generate the wide range of operating conditions with uncertainty. Therefore, probabilistic approaches can be used by alleviating the drawbacks of deterministic approach as follows.

1. The Risk based security index is calculated using uncertainty of operating conditions and contingencies. The severity function is used to represent the true impact on the power system in the specified conditions such as contingencies. Therefore, risk based security index gives better quantitative evaluation of the power system than deterministic approach.

The severity function is used to capture the performance of operating parameters such as voltage, line flow, and stability margin after being subjected to severe disturbances. Full description of the severity function is given in the Section 2.4.2.

2. Severity function is used to introduce the economic impact on the power system.

3. It captures the increased risk caused by the multiple contingencies as it sums the risk associated with all contingencies.

4. The severity function considers the uncertainty in operating conditions.

5. The risk index is a composite index that considers all probable contingencies weighted by their probability of occurrence during the considered time period.

2.3 Dynamic Security Assessment

The dynamic security assessment determines whether the power system reaches a new equilibrium operating point or not after the transition. As indicated in Figure 1.1 the dynamic security assessment can be categorized into transient stability and oscillatory stability security assessment. In this thesis, dynamic security assessment based on the transient stability is considered.

Transient stability is the ability of the power system to maintain synchronism when subjected to a severe transient disturbances. The resulting system response involves large excursions of generator rotor angels and is influenced by the nonlinear power angle relationship. Transient stability depends both on the initial operating state of the power system and severity of the disturbance. Usually, the system is altered so that the post-disturbance steady-state operation differ from that prior to the disturbance [6].

In general, security analysis deals with the power system's response to disturbances. In steady state analysis, the transition to a new operating condition is assumed to have taken place, and the analysis is aimed to ensure that operating constraints such as thermal and voltage limits are met. In dynamic security assessment the transition itself is of interest, i.e. the analysis checks whether the transition will lead to new equilibrium operating point. As a result of loss of dynamic stability, conditions such as loss of synchronism of some generators, transient voltage at a key bus falling below a certain level and operation of an out of step relay resulting in the opening of a heavy loaded tie line might be happen [23].

2.4 Risk Based Security Assessment

2.4.1 Risk

The risk is the systems exposure to failure and obtained by considering both the probability of occurrence of an event and the impact of the event. The deterministic security assessment introduces operating limits based on the impact of contingencies. However, according to the risk based approach proposed in [24], these operating limits are calculated by getting weighted sum of risk components of all the contingencies in the list considering both the probability and the impact.

The glass factory example presented in Chapter 1 is modified to understand the risk based approach for two operating conditions. The best operating condition is selected by comparing the risk levels. The accidents are equivalent to the power system contingencies and different machines are equivalent to the power system operating conditions. Consider the data given in Table 2.1. There are two machines with deferent probability levels for deferent accidents. The basic risk Equation 1.1 in Chapter 1 is used to calculate the composite risk. From the results the machine 1 is less risky than machine 2 and machine 1 is selected for bottle production.

If deterministic approach is used to select the suitable machine, first severe accident should be selected. The accident II is the most severe one. The machine 1 damages more bottles with accident II. Therefore, machine 2 is selected for bottle production.

Table 2.1: Risk values for two Accidents for different operating conditions

Event	Machine 01		Machine 02	
	Probability	Impact	Probability	Impact
Accident I	0.05	20	0.07	20
Accident II	0.02	30	0.01	25
Risk		**1.60**		**1.65**

In traditional deterministic security assessment, the performance of the power system under a given set of contingencies is assessed using standard tools such as power flow and stability simulation programs. Furthermore, in deterministic security analysis the probability of these contingencies are not directly taken into account. Although these contingencies are the most probable contingencies amongst all possible contingencies, they are not equally probable. There could also be contingencies that are not in the selected set of contingencies although they have a significant impact on the operation of a power system, because the probability of their occurrence is very low. Deterministic approach ignores these contingencies. These shortcomings of the present practice could be overcome if risk based security analysis techniques applicable to large power systems could be developed.

The work presented in this thesis extends the static security assessment technique in [8] to calculate risk based dynamic security indices using the polynomial form of the transient stability margin given in [9].

The glass factory example can be developed to equivalent with real power system risk calculations. In this case, two machines are operating in a glass factory with different availability levels as indicated in Table 2.2. The total risk of the glass factory is 2.315 bottles per day.

Table 2.2: Total Risk for the glass factory with two different machines with two accidents

Event	Machine 01		Machine 02	
	Probability	Impact	Probability	Impact
Availability	0.80		0.70	
Accident I	0.05	20	0.07	20
Accident II	0.02	25	0.01	25
Risk		1.2		1.115
Total Risk				**2.315**

The real power system example consists with contingencies (equivalent to accident in glass factory), operating conditions (equivalent to machines) and severity functions (equivalent to number of damaged bottles per accident). The probability of the power system operating conditions such as load P and Q are represented by the normal distribution. The probability of the contingencies are represented by Poisson distribution. The real power system risk calculation procedure is explained as follows:

The risk index is defined in [8] as an expectation of severity, computed by adding overall possible outcomes of the product of probability of an event and its severity. If we assign probabilities to each branch of Figure 2.1, then the probability of each terminal state is the product of the probabilities assigned to the branches that connect the initial state to that terminal state.

The total system risk can be calculated by multiplying individual risk components by probabilities of each contingency for a particular forecast condition using Equation

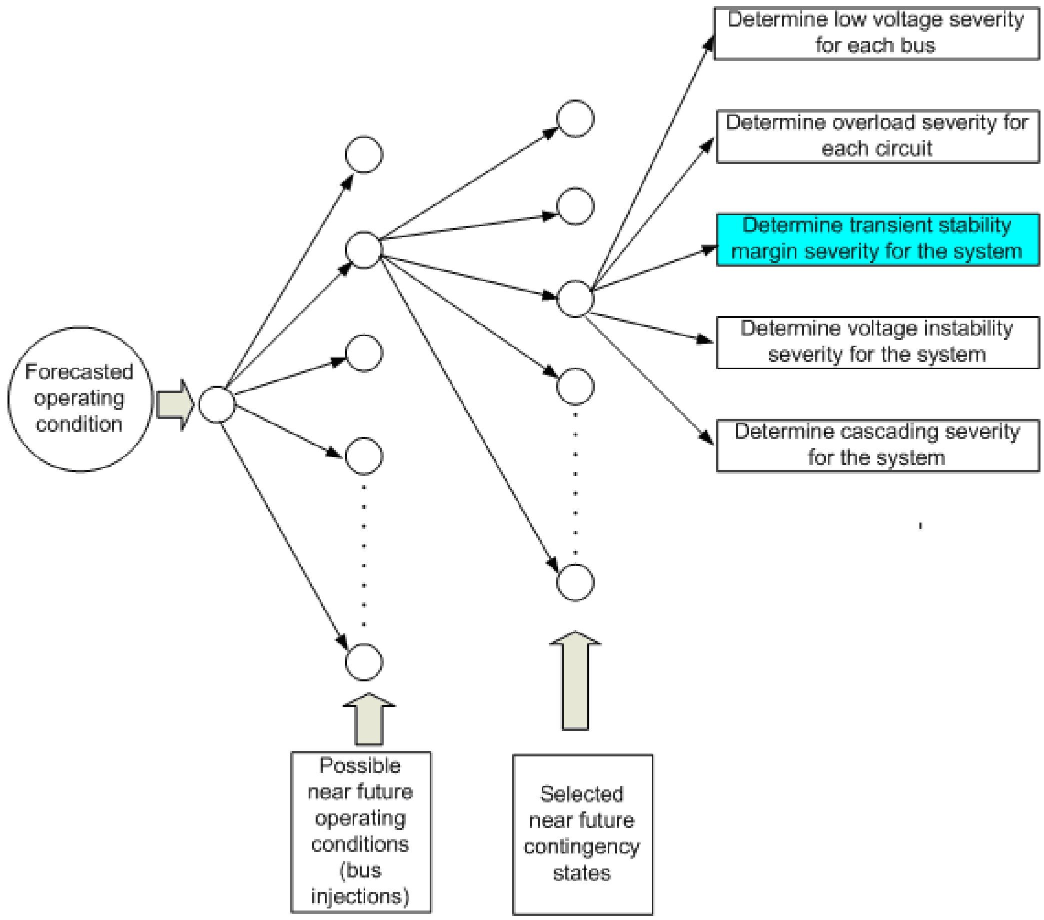

Figure 2.1: Risk based security assessment calculation.

(2.1).

$$Risk(SM_{t,f}) = \sum_i \Pr(E_i)\left[\sum_j Pr(SM/E_i, X_{t,f}) \times Sev(E_i, X_{t,f})\right] \tag{2.1}$$

where,

1. $X_{t,f}$: forecast uncertain loading condition at time t.

2. $Pr(SM/E_i, X_{t,f})$: probability of the stability margin for i^{th} contingency and

forecast uncertain loading condition.

3. $Pr(E_i)$: probability of i^{th} contingency.

4. $Sev(E_i, SM)$: severity function which quantify the impact of the i^{th} contingency with variation of stability margin.

For the mathematical formulation of risk calculation of stability margin, Equation (2.1) can be rewritten in integral form as in Equation (2.2).

$$Risk(SM_{t,f}) = \sum_i \Pr(E_i) \left[\int_{-\infty}^{\infty} Pr(SM/E_i, X_{t,f}) \times Sev(E_i, SM) dSM \right] \tag{2.2}$$

where,

1. $X_{t,f}$: forecast uncertain loading condition at time t.

2. $Pr(SM/E_i, X_{t,f})$: probability of the stability margin for i^{th} contingency and forecast uncertain loading condition.

3. $Pr(E_i)$: probability of i^{th} contingency.

4. $Sev(E_i, SM)$: severity function which quantify the impact of the i^{th} contingency with variation of stability margin.

2.4.2 Severity

The severity function is used to capture the risk associated with the stability margin after being subjected to severe disturbances. For risk calculations, continuous severity function presented in Figure 2.2 is selected as it produces most realistic distinguishable results for different contingencies than other severity models used in the literature [8, 11], such as, discrete severity function. The stability margin can be defined as difference between critical clearing time(CCT) and actual clearing time. The CCT is the maximum time interval that the power system fault should be cleared keeping the power system transiently stable. The actual clearing time is the fault clearing time from the power system protection system.

The severity function for the stability margin is defined by considering the CCT and actual clearing time. When the CCT is greater than the actual clearing time, there is no risk (i.e. risk is low). If the CCT is smaller than the actual clearing time, then there is a risk. The continuous severity function shown in Figure 2.2 is chosen so that, the larger the difference between the CCT and actual clearing time, the larger the associated risk. From practical point of view, this makes more sense than a discrete severity function that treats all situations where CCT is smaller than the actual clearing time as equally bad. In a real system, the longer the fault clearing is delayed, the more wide spread and severe the effect would be. The per unit (pu) system is developed to ease the calculation. It is considered the fact: 1.0 pu CCT is equivalent to the 8 cycles of IEEE 39 bus test system, which is around to be the actual clearing time. The severity is 1.0 for 0.997 pu CCT and 0.0 when CCT is greater than or equal to 1.0 pu and linearly increases when CCT decreases from 1.0 pu.

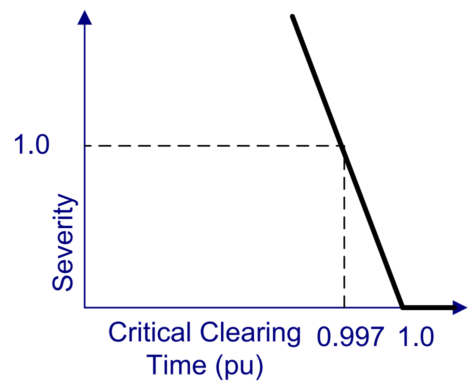

Figure 2.2: Continuous severity function

2.4.3 Uncertainty of operating condition

In this thesis, the linear approximation techniques developed in the risk based static security assessment in [8] are extended to implement the risk based dynamic security assessment. Uncertainty of stability margin is modeled by joint-probability density function ($Pr(SM/E_i, X_{t,f})$) that provides the probability of stability margin (SM) to forecast uncertain load condition at time **t**, ($X_{t,f}$) for the i^{th} contingency. The probability distribution of the transient stability margin is obtained by introducing uncertain loading condition to the IEEE 39 bus test system. The procedure of obtaining the probability distribution of the stability margin is explained below.

It is assumed that P and Q of load buses are normally distributed with forecast base case mean value and defined standard deviation. The small deviation for load P and Q is selected to make valid linear approximations in the sensitivity calculations. These sensitivities are used to obtain the probability distribution of the stability margin. The voltage V and the voltage angle δ of each bus of the study system depend on the behavior of all load P and Q and this will lead to multivariate normal distribution of V and δ. The stability margin is defined as a function of all V and δ of the study system for a particular contingency in [9]. Using this function, the stability margin can be calculated for any operational values of V and δ of all the buses for any contingency. The probability distribution of the stability margin is obtained by using the multivariate normally distributed V and δ with functional form of the stability margin. Therefore, stability margin also follows the normal distribution. For a particular contingency, transient stability margin in functional form is used to calculate the partial derivatives of the stability margin with respect to V and δ of all buses. These partial derivatives are calculated by differentiating the transient stability margin polynomial with respect to power flow variables V and δ. The mean value of the transient stability margin for the k^{th} contingency is obtained from transient stability margin polynomial, and required inputs ($V and\ \delta$) for the mean value calculation are obtained from the base case standard load flow solution. The standard deviation of the stability margin is calculated using the sensitivities, and variance-covariance matrix of load P and Q, and the procedure of obtaining the standard deviation is explained below. Then, probability distribution of stability margin is modeled as a normal distribution using Equation (2.3) according to the linear approximation model given in [8].

$$SM_k \approx\ N\left(E(SM_k), (S_p^T \times V_p \times S_p)\right) \tag{2.3}$$

The sensitivities S_p are calculated from both partial derivatives of stability margin with respect to ($V and\ \delta$), and partial derivatives from standard load flow Jacobian matrix. The available transient stability margin polynomial in [9] is differentiable and all the required sensitivities can be calculated. The variance covariance matrix can be obtained from historical data.

In conclusion, the risk based security assessment presented in this section confirm that proposed method can be used to address the problems associated with deterministic security assessment. This method helps to get good understanding about the risk of the operation of stressed power system under uncertain conditions. However, to cope with dynamic behavior of different component of the power system, the risk based dynamic security assessment should be done by considering the uncertainty of operating conditions and contingency.

2.5 Concluding Remarks

The methods of deterministic and probabilistic security assessment have been presented in this chapter. The disadvantages of deterministic approach and the methods of eliminating these problems with probabilistic approach have been discussed. The concept of the risk has been discussed with uncertainty and severity. The concept of Risk based security assessment have been introduced and the way this method could be developed for risk based dynamic security assessment has been presented.

Chapter 3

Risk Based Static Security Assessment

3.1 Introduction

As concluded in Chapter 2 the probabilistic security assessment is essential to calculate the actual security level of the power system under uncertain operating conditions. The risk based security index can be evaluated to get a good understanding about the cost of the risk and it can be used to do security-economy decision making at the control room environment. The risk based optimal power flow is developed in [25], and a monetary value was introduced for each risk component such as line overload and voltage out of limits. The risk components have been used as constrains of optimal power flow. The basic idea of risk based security assessment of power systems have been developed at Iowa State University from 1994. Different types of risk based static security assessment approaches for various security problems have been discussed in [8, 10, 11, 20, 21, 24].

The risk based static security assessment basics have been discussed in this chapter with low voltage and line overload associated with uncertain operating conditions. The IEEE New England 39 bus test system [26] is used to demonstrate the calculation of the risk indices with two contingencies. The linear approximation method is used to calculate the risk indices, and then validated against non linear model using Monte Carlo simulation techniques. Various sensitivities are required to find the probability distribution of bus voltages and line flows. All the sensitivities are developed from the basics of power flow. A number of mathematical techniques such as matrix manipulations to get required sensitivities from Jacobian matrix and standard deviation calculation from variance-covariance matrix with other sensitivities (described in Section 3.3.1) are used to get the final probability distribution.

3.2 Newton Raphson Power Flow

In this chapter, the probability distribution of voltage and line flow have been obtained when the operating conditions are uncertain. The active power P and reactive power Q of load buses are selected as uncertain operating parameters, and it is assumed that they are normally distributed with the base case mean value and a known standard deviation. The different standard deviation values of P and Q are selected to check the accuracy of the linear model with the non-linear model simulated using the Monte Carlo simulation. To calculate the probability distribution of voltage, different types of sensitivities of that particular voltage are required with respect to P and Q of all the load buses. These sensitivities can be obtained from the Newton Raphson power flow Jacobian matrix and the variance-covariance matrix. The procedure of obtaining these sensitivities for static security assessment is described in the following sections.

3.2.1 Power Flow

In the power flow problem, real power P and voltage magnitude V are specified for generator buses with voltage control capability. The power flow equations are formulated in polar form as presented in [27]. For the simplified power system shown in the Figure 3.1, following power flow equations can be written.

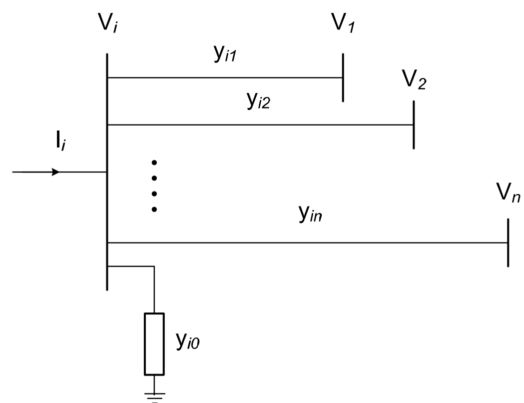

Figure 3.1: Typical bus of the power system.

The current entering into bus i is given by

$$I_i = \sum_{j=1}^{n} Y_{ij} V_j \tag{3.1}$$

where, Y_{ij} is the i^{th} row j^{th} column element of the bus admittance matrix.

Equation (3.1) in Polar form

$$I_i = \sum_{j=1}^{n} |Y_{ij}||V_j| \angle(\theta_{ij} + \delta_j) \tag{3.2}$$

where, δ_j : voltage angle, θ_{ij} : angle of elements of bus admittance matrix.

The complex power at bus i is given by

$$P_i - jQ_i = V_i^* I_i \tag{3.3}$$

From Equations (3.1), (3.2) and (3.3)

$$P_i - jQ_i = |V_i|\angle{-\delta_i} \sum_{j=1}^{n} |Y_{ij}||V_j|\angle(\theta_{ij} + \delta_j) \tag{3.4}$$

By separating real and imaginary parts,

$$P_i = \sum_{j=1}^{n} |V_i||V_j||Y_{ij}|cos(\theta_{ij} - \delta_i + \delta_j) \tag{3.5}$$

$$Q_i = -\sum_{j=1}^{n} |V_i||V_j||Y_{ij}|sin(\theta_{ij} - \delta_i + \delta_j) \tag{3.6}$$

Equations (3.5) and (3.6) constitute a set of non-linear algebraic equations in terms of the independent variables, voltage magnitude in *per unit* and phase angle in *radians*. Following equations can be written for load and generator buses.

Two equations: for each load bus using Equations (3.5) and (3.6)

One equation: for generator bus with voltage control using Equation (3.5)

By expanding Equations (3.5) and (3.6) using Taylor series around the initial estimate and neglecting all higher order terms results in the following set of linear equations.

$$\left[\begin{array}{c} \Delta P_2^k \\ \vdots \\ \Delta P_n^k \\ \hline \Delta Q_2^k \\ \vdots \\ \Delta Q_n^k \end{array}\right] = \left[\begin{array}{ccc|ccc} \frac{\partial P_2^k}{\partial \delta_2} & \cdots & \frac{\partial P_2^k}{\partial \delta_n} & \frac{\partial P_2^k}{\partial |V_2|} & \cdots & \frac{\partial P_2^k}{\partial |V_n|} \\ \vdots & & & & & \\ \frac{\partial P_n^k}{\partial \delta_2} & \cdots & \frac{\partial P_n^k}{\partial \delta_n} & \frac{\partial P_n^k}{\partial |V_2|} & \cdots & \frac{\partial P_n^k}{\partial |V_n|} \\ \hline \frac{\partial Q_2^k}{\partial \delta_2} & \cdots & \frac{\partial Q_2^k}{\partial \delta_n} & \frac{\partial Q_2^k}{\partial |V_2|} & \cdots & \frac{\partial Q_2^k}{\partial |V_n|} \\ \vdots & & & & & \\ \frac{\partial Q_n^k}{\partial \delta_2} & \cdots & \frac{\partial Q_n^k}{\partial \delta_n} & \frac{\partial Q_n^k}{\partial |V_2|} & \cdots & \frac{\partial Q_n^k}{\partial |V_n|} \end{array}\right] \left[\begin{array}{c} \Delta \delta_2^k \\ \vdots \\ \Delta \delta_n^k \\ \hline \Delta |V_2^k| \\ \vdots \\ \Delta |V_n^k| \end{array}\right] \tag{3.7}$$

The above equations are written such that, bus 1 is selected as the slack bus. The Jacobian matrix gives the linearized relationship between small changes in voltage angle $\Delta\delta_i^k$ and voltage magnitude $\Delta|V_i^k|$ with the small change in real and reactive power ΔP_i^k and ΔQ_i^k. The elements of Jacobian matrix are the partial derivative of Equations (3.5) and (3.6). The above equation can be rewritten as,

$$\begin{bmatrix} \Delta P \\ \Delta Q \end{bmatrix} = \begin{bmatrix} J1 & J2 \\ J3 & J4 \end{bmatrix} \begin{bmatrix} \Delta\delta \\ \Delta|V| \end{bmatrix} \tag{3.8}$$

In the case of generator buses, the voltage magnitudes are known and do not required to be calculated. Therefore, if m buses of the system are generator buses, m equations involving ΔQ and ΔV and corresponding columns of Jacobian matrix are eliminated. There are *(n-1)* real power constraints and *(n-1-m)* reactive power constraints due to elimination of slack bus and voltage controlled buses. The Jacobian matrix is of the order of *(2n-2-m)x(2n-2-m)*, and individual sub matrices have the order of,

J1:-(n-1)x(n-1),

J2:-(n-1)x(n-1-m),

J3:-(n-1-m)x(n-1) and

J4:-(n-1-m)x(n-1-m).

The elements of Jacobian matrix are as follows,

J1:

Diagonal

$$\frac{\partial P_i}{\partial \delta_i} = \sum_{j \neq i} |V_i||V_j||Y_{ij}|sin(\theta_{ij} - \delta_i + \delta_j) \tag{3.9}$$

Off-diagonal

$$\frac{\partial P_i}{\partial \delta_j} = -|V_i||V_j||Y_{ij}|sin(\theta_{ij} - \delta_i + \delta_j) \qquad for j \neq i \tag{3.10}$$

J2:

Diagonal

$$\frac{\partial P_i}{\partial |V_i|} = 2|V_i||Y_{ij}|\cos\theta_{ii} + \sum_{j \neq i} |V_j||Y_{ij}|cos(\theta_{ij} - \delta_i + \delta_j) \tag{3.11}$$

Off-diagonal

$$\frac{\partial P_i}{\partial |V_j|} = |V_i||Y_{ij}|cos(\theta_{ij} - \delta_i + \delta_j) \qquad for j \neq i \tag{3.12}$$

J3:

Diagonal

$$\frac{\partial Q_i}{\partial \delta_i} = \sum_{j \neq i} |V_i||V_j||Y_{ij}|cos(\theta_{ij} - \delta_i + \delta_j) \tag{3.13}$$

Off-diagonal

$$\frac{\partial Q_i}{\partial \delta_j} = -|V_i||V_j||Y_{ij}|cos(\theta_{ij} - \delta_i + \delta_j) \qquad for j \neq i \tag{3.14}$$

J4:

Diagonal

$$\frac{\partial Q_i}{\partial |V_i|} = -2|V_i||Y_{ij}|\sin\theta_{ii} - \sum_{j \neq i} |V_j||Y_{ij}|sin(\theta_{ij} - \delta_i + \delta_j) \tag{3.15}$$

Off-diagonal

$$\frac{\partial Q_i}{\partial |V_j|} = -|V_i||Y_{ij}|sin(\theta_{ij} - \delta_i + \delta_j) \qquad for j \neq i \tag{3.16}$$

If the difference between the scheduled and calculated values of P and Q are ΔP_i^k and ΔQ_i^k. It is also known as residuals, which is given by,

$$\Delta P_i^k = P_i^{sch} - P_i^k \tag{3.17}$$

$$\Delta Q_i^k = Q_i^{sch} - Q_i^k \tag{3.18}$$

The new bus voltages can be estimated as,

$$\delta_i^{k+1} = \delta_i^k + \Delta\delta_i^k \tag{3.19}$$

$$V_i^{k+1} = V_i^k + \Delta V_i^k \tag{3.20}$$

The above equations can be used to find the solution for the power flow problem. The calculation process is continued until the residuals ΔP_i^k and ΔQ_i^k are less than the specified tolarance. The required sensitivities for probability calculation are obtained from the Jacobian matrix.

3.2.2 Line Flow

The bus voltages and the voltage angles are obtained from the final converged solution of the power flow. These voltages and voltage angles are used to calculate the line flows and line losses. The line flow sensitivities with respect to V and δ of terminal bus voltages are required to calculate the probability distribution of the line flow. Lets consider a line connecting two buses i and j as shown in Figure 3.2.

Equations for current flowing through lines can be written as follows.

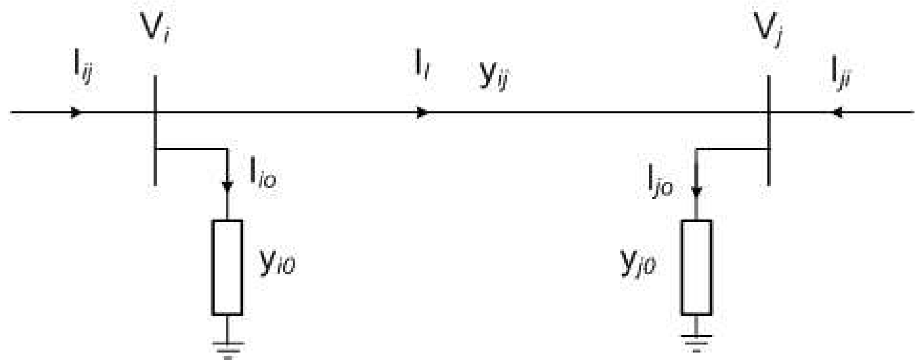

Figure 3.2: Simple Transmission line model

Line flow from i to j

$$I_{ij} = I_l + I_{io} = y_{ij}(V_i - V_j) + y_{io}V_i \tag{3.21}$$

Line flow from j to i

$$I_{ji} = -I_l + I_{jo} = y_{ij}(V_j - V_i) + y_{io}V_j \tag{3.22}$$

The complex power is given by,

From bus i to j

$$S_{ij} = V_i I_{ij}^* \tag{3.23}$$

Form bus j to i

$$S_{ji} = V_j I_{ji}^* \tag{3.24}$$

By separating the real and reactive power components, the real power flow along the line can be written as,

$$P_{ij} = V_i^2 Y_{ij} cos(\theta ij) - V_i V_j cos(\theta_{ij} - \delta_i + \delta_j) + V_i^2 Y_{io} cos(\theta_{io}) \tag{3.25}$$

By taking the partial derivatives with respect to V and δ of the two ends of the line

$$\frac{\partial P_{ij}}{\partial |V_i|} = 2|V_i||Y_{ij}|cos(\theta_{ij}) - |V_j|cos(\theta_{ij} - \delta_i + \delta_j) + 2|V_i||Y_{io}|cos(\theta_{io}) \;\; for j \neq i \quad (3.26)$$

$$\frac{\partial P_{ij}}{\partial |V_j|} = -|V_i|cos(\theta_{ij} - \delta_i + \delta_j) \qquad for j \neq i \quad (3.27)$$

$$\frac{\partial P_{ij}}{\partial \delta_i} = -|V_i||V_j||Y_{ij}|sin(\theta_{ij} - \delta_i + \delta_j) \qquad for j \neq i \quad (3.28)$$

$$\frac{\partial P_{ij}}{\partial \delta_j} = |V_i||V_j||Y_{ij}|sin(\theta_{ij} - \delta_i + \delta_j) \qquad for j \neq i \quad (3.29)$$

By using Equations (3.26), (3.27), (3.28) and (3.29), line flow sensitivities with respect to V and δ of the terminal buses are calculated.

3.3 Risk Based Voltage Security Assessment - Linearized Method

The probability distribution of voltage of each bus, probability of each contingency and defined severity functions are required to carry out the risk based voltage security assessment. The procedure of obtaining and defining above values and models are explained in the following sections. The probability distribution of voltages as in Equation 3.36 are obtained from linearized method, and risk indices are calculated using Equation 3.39. These risk indices are also compared with those estimated by Monte Carlo simulation for the non-linear model.

3.3.1 Uncertainty of Operating Condition

The Jacobian matrix (J) is obtained at the beginning of this chapter, and it contains sensitivities of P and Q with respect to V and δ. However, for the voltage risk calculation, sensitivities of V with respect to P and Q are required. These sensitivities can be obtained by simply inverting the Jacobian matrix. On the other hand, computing the inverse Jacobian matrix requires more computing power for large power systems. Therefore, special techniques can be implemented to overcome this problem. Fortunately, in low voltage risk assessment, it is not required to assess the risk of all buses. The requirement is to evaluate the low voltage risk of stressed buses having voltage magnitude lower than the specified value. Therefore, only need to calculate the sensitivities of stressed buses' voltages with respect to load bus P and Q. The sensitivities of particular voltage are located at the particular row of J^{-1}. Therefore, only need to find that particular rows for the stressed buses. The row of J^{-1} can be obtained using following technique without inverting the Jacobian matrix.

As an example, for a matrix A, if i^{th} column of the A^{-1} is required, it can be obtained by solving the following linear equation,

$$A \times x = b \tag{3.30}$$

Where b is the column vector such that all of the elements of b equal to 0 except $b_i = 1$. The solution x is the i^{th} column vector of A^{-1}.

However, the requirement of the application is a row of A^{-1} and not a column. Therefore, first transpose of A (i.e.A^T) is obtained. Then, i^{th} column of A^T is calculated using above technique. Finally, transpose of this column vector is obtained, and it is the required row vector of the A^{-1} matrix.

The Jacobian matrix J obtained from Newton Rapson power flow is given in

Equation(3.31).

$$[J] = \left[\begin{array}{ccc|ccc} \frac{\partial P_2}{\partial \delta_2} & \cdots & \frac{\partial P_2}{\partial \delta_n} & \frac{\partial P_2}{\partial |V_2|} & \cdots & \frac{\partial P_2}{\partial |V_n|} \\ \vdots & & & & & \\ \frac{\partial P_n}{\partial \delta_2} & \cdots & \frac{\partial P_n}{\partial \delta_n} & \frac{\partial P_n}{\partial |V_2|} & \cdots & \frac{\partial P_n}{\partial |V_n|} \\ \hline \frac{\partial Q_2}{\partial \delta_2} & \cdots & \frac{\partial Q_2}{\partial \delta_n} & \frac{\partial Q_2}{\partial |V_2|} & \cdots & \frac{\partial Q_2}{\partial |V_n|} \\ \vdots & & & & & \\ \frac{\partial Q_n}{\partial \delta_2} & \cdots & \frac{\partial Q_n}{\partial \delta_n} & \frac{\partial Q_n}{\partial |V_2|} & \cdots & \frac{\partial Q_n}{\partial |V_n|} \end{array}\right] \tag{3.31}$$

The required row of J^{-1} can be obtained from above mentioned technique. After screening all busses, the stressed voltage buses are identified. If one of the stressed voltage bus is i^{th} bus, then sensitivity vector S_p for the probability calculation is given in Equation (3.32).

$$[S_p] = \left[\begin{array}{c} \frac{\partial V_i}{\partial P_2} \\ \vdots \\ \frac{\partial V_i}{\partial P_n} \\ \hline \frac{\partial V_i}{\partial Q_2} \\ \vdots \\ \frac{\partial V_i}{\partial Q_n} \end{array}\right] \tag{3.32}$$

The probability distribution of the stressed bus voltage V_i need to be obtained using derived sensitivities. From the basic theory developed for risk based security assessment in [8], it is assumed that the voltage also follows a normal distribution with normally distributed load P and Q. The mean voltage value of the probability distribution is equal to the base case voltage value for relatively small deviations. To obtain the standard deviation of V_i, sensitivity of V_i with respect to uncertain operation parameters and variance-covariance matrix of the uncertain operating parameters are required. For the work presented in this thesis, loads P and Q are selected as uncertain operating parameters. For the New England IEEE 39 bus test system, there are 29 load buses (nL) and therefore, variance-covariance matrix is a, 58×58 matrix. The variance-covariance matrix (C_p) can be obtained from historical data for real control room calculations and assumed variance-covariance matrix have been used here to illustrate the calculation procedure. The assumed variance-covariance matrix is calculated using forecast load value and assumed load standard deviation. The diagonal elements of the variance-covariance matrix are obtained by getting the square of the product of the load and load standard deviation. It is assumed that non-diagonal elements are zero as there is no dependence between loads on different buses. Also, for the calculation, it is assumed that the different load standard deviations from 1% to 10%. The variance-covariance matrix is given in Equation (3.33).

$$[C_p] = \begin{bmatrix} \sigma_{P_1}^2 \; \ldots & 0 & 0 \; \ldots & 0 \\ \vdots & & & \\ 0 \; \ldots & \sigma_{P_{nL}}^2 & 0 \; \ldots & 0 \\ 0 \ldots & 0 & \sigma_{Q_1}^2 \; \ldots & 0 \\ \vdots & & & \\ 0 \ldots & 0 & 0 \; \ldots & \sigma_{Q_{nL}}^2 \end{bmatrix} \tag{3.33}$$

From Equations (3.32) and (3.33), the variance of the voltage V_i can be written as presented in Equation (3.34).

$$[\gamma_{V_i}] = \begin{bmatrix} \frac{\partial V_i}{\partial P_1} & \dots & \frac{\partial V_i}{\partial P_{nL}} & \frac{\partial V_i}{\partial Q_1} & \dots & \frac{\partial V_i}{\partial Q_{nL}} \end{bmatrix} \times \begin{bmatrix} \sigma^2_{P_1} \dots & 0 & 0 \dots & 0 \\ \vdots & & & \\ 0 \dots & \sigma^2_{P_{nL}} & 0 \dots & 0 \\ 0 \dots & 0 & \sigma^2_{Q_1} \dots & 0 \\ \vdots & & & \\ 0 \dots & 0 & 0 \dots & \sigma^2_{Q_{nL}} \end{bmatrix} \times \begin{bmatrix} \frac{\partial V_i}{\partial P_1} \\ \vdots \\ \frac{\partial V_i}{\partial P_{nL}} \\ \frac{\partial V_i}{\partial Q_1} \\ \vdots \\ \frac{\partial V_i}{\partial Q_{nL}} \end{bmatrix} \tag{3.34}$$

Then the standard deviation can be obtained from the variance,

$$\sigma_{V_i} = \sqrt{\gamma_{V_i}} \tag{3.35}$$

According to the initial assumption, V_i is normally distributed and therefore, probability distribution of V_i is,

$$Pr(V_i) = \frac{1}{\sigma_{V_i}\sqrt{2\pi}}\, e^{-\frac{(V_i-\mu_{V_i})^2}{2\sigma^2_{V_i}}} \tag{3.36}$$

This probability distribution can be used to calculate the risk with the defined severity function.

3.3.2 Uncertainty of Contingency

The traditional power industry practice is to consider impact of each contingency, but not the probability of them during security assessments. Therefore, in deterministic security assessment, decisions are taken based on the most severe contingency. In power systems, contingencies are caused by the failure of one or more components such as a generator, a transformer or a transmission line. The failure statistics of different components have different failure rates. The generator failure rates given in [28] depend on the capacity of generators. The failure rates of transmission lines vary with their voltage ratings as high voltage lines have low failure rates than medium voltage lines.

The Poisson distribution can be used to model the probability distribution of the contingency as it is a rare event [8]. The probability distribution of Poisson distribution is given in Figure 3.3 for different λ values. Where λ is the mean number of events during a given unit of time.

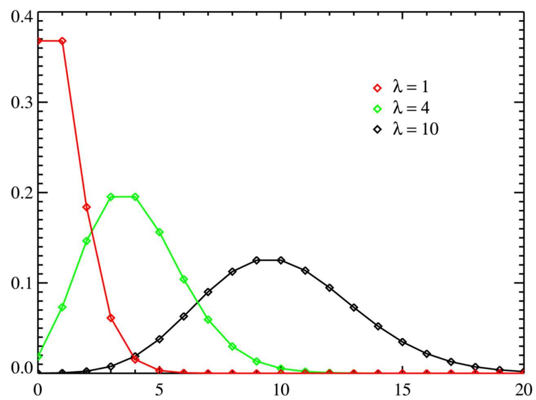

Figure 3.3: Poisson distribution for different λ

The formula for Poisson distribution is,

$$Pr(x) = \frac{\lambda^x e^{-\lambda}}{x!} \qquad x = 0, 1, 2 \ldots \tag{3.37}$$

where λ is the mean number of events during a given unit of time

x is the number of occurrence

The occurrence rate of the contingency for a year can be obtained from the historical data of the utility company, and occurrence rate for a hour can be obtained by dividing it by 8760. The probability of a certain contingency is the probability that contingency occurs at least one time in next hour, and it can be represented as,

$$Pr(E_i) = \sum_{x=1}^{\infty} Pr(x) = 1 - Pr(x = 0) = 1 - e^{-\lambda_i} \tag{3.38}$$

where, λ_i is the occurrence rate of contingency i per time interval.

3.3.3 Severity

As described in Chapter 2, the severity function is used to capture the risk associated with uncertain operating parameters, such as voltage or transient stability margin after being subjected to a severe disturbance. For risk calculations, continuous severity function as in Figure 2.2 is selected because it produces most realistic distinguishable results for different contingencies than other severity models (e.g. discrete severity function) used in the literature [8, 11].

In [8], good features of severity function that can be used for each security problem in risk based security assessment have been identified. The good features that should be incorporated with severity function are,

I. The severity function should reflect the consequences of contingency and loading condition rather than operator's decision. When the operator initiate the load curtailment or re-dispatch, it is a consequence of operator's decision rather than power system's behavior.

II. The severity for contingencies should reflect consequences that are physically understandable in terms of network parameters by the operator. This ensures that the generated risk indices reflect quantitative evaluation to see the insight of the problem operators face.

III. In order to facilitate the transition from deterministic approaches to probabilistic decision making, the severity function should be tied to the deterministic decision criteria to the extent possible.

IV. The severity function should be as simple as possible.

V. The severity function should reflect the relative severity between different problems to enable calculation of the composite indices.

VI. The severity function should measure the extent of the violation.

The different types of severity functions are available and each has its own strength and weaknesses. The severity function is defined in terms of network performance measures such as voltage, line flow and transient stability margin.

1. Severity function for low voltage: The severity functions for each and every buses are defined separately and the magnitude of the voltage of that particular bus defines the severity value for that bus. There are two popular types of severity functions for the low voltage risk calculations.

a.) *Discrete Severity Function*: Severity is 1.0 if the voltage is below the rated voltage and otherwise severity is zero. See Figure 3.4a. This model is very simple and have strong coupling with deterministic approach. But this function does not reflect the extent of the violation.

b.) *Continuous Severity Function*: The severity is 0.0 when voltage is 1.0pu or high and linearly increase when the voltage decreases. The severity is 1.0 for each bus when the voltage is at 0.95pu. See Figure 3.4b. This severity function reflects the extent of violation.

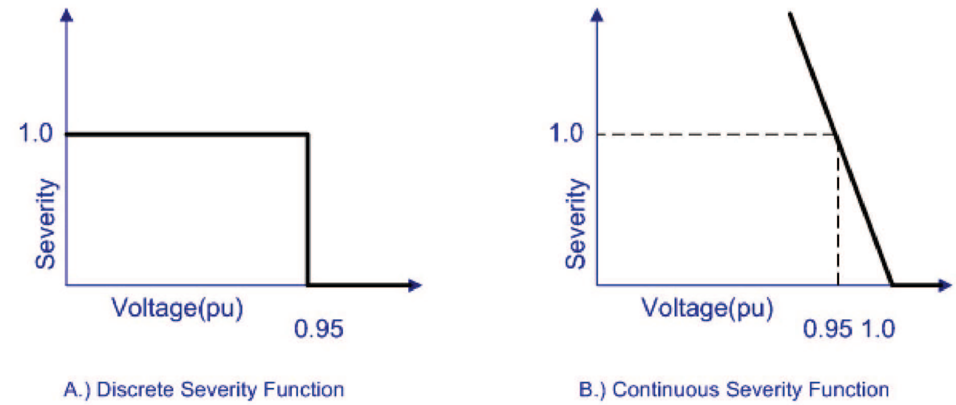

Figure 3.4: Severity Function for low voltage

2. **Severity function for overload:** As in the same way in the voltage case, severity function is defined for each transmission line. The percentage of rating for each line is defined as the ratio between real load and rated load. The specific severity function is defined for each circuit. The continuous and discrete severity functions can be used for risk calculation. See Figure 3.5.

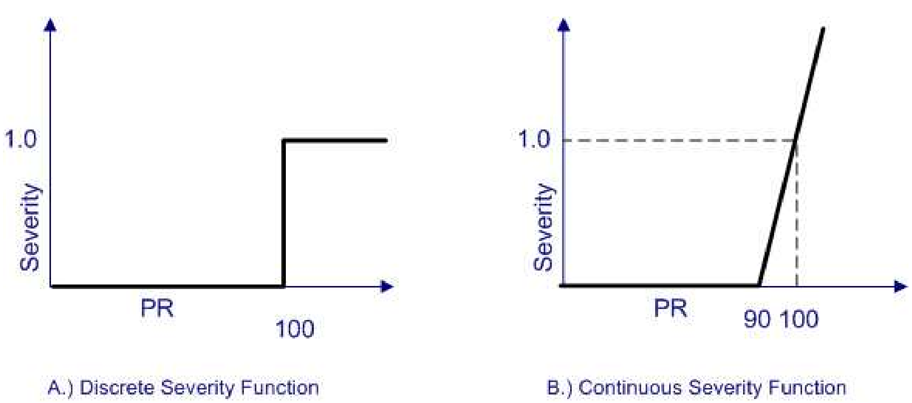

Figure 3.5: Severity Function for over load

3. **Severity function for transient stability margin:** For transient stability margin risk calculation, continuous severity function is selected as it produces most

desirable results than other severity models used. When the critical clearing time (CCT) is greater than the actual clearing time, there is no risk (i.e. risk is low). If the CCT is smaller than the actual clearing time, then there is a risk. The continuous severity function shown in Figure 3.6 is chosen so that, the larger the difference between the CCT and actual clearing time, the larger the associated risk. From practical point of view this make more sense than a discrete severity function that treats all situations where CCT is smaller than the actual clearing time as equally bad. In a real system, the longer the fault clearing is delayed, the more wide spread and severe the effect will be. The pu system is developed to ease the calculation and 1.0 pu CCT is equivalent to the 8 cycles of IEEE 39 bus test system, which is around to be the actual clearing time. The severity is 1.0 for 0.997 pu CCT and 0.0 when CCT is greater than or equal to 1.0 pu and linearly increases when CCT decreases from 1.0 pu. The continuous severity functional model used for risk calculation is indicated in Figure 3.6.

3.3.4 Risk Calculation Procedure

The probability distribution of the voltage of stressed buses are obtained according to the Section 3.3.1, and continuous severity function is defined as described Section 3.3.3. By multiplying these two functions together and then calculating the area under the resultant curve gives the risk index for particular stressed bus for specific contingency. The risk indices of all the stressed buses are added together and multiplied by the probability of contingency. Equation (2.1) in Chapter 2 can be modified and used to calculate the total low voltage risk for all probable contingencies by using Equation (3.39). The resultant curve of probability distribution of voltage for one

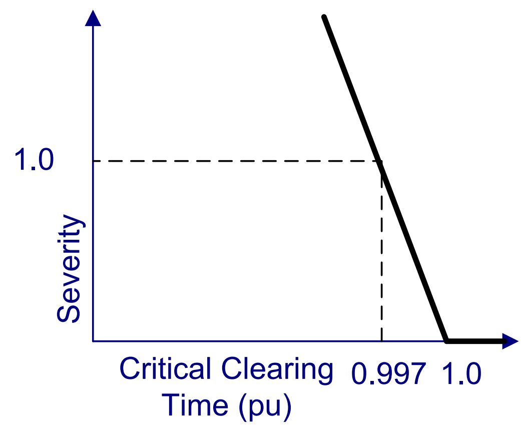

Figure 3.6: Continuous severity function for transient stability margin

bus is given in Figure 3.7 with severity function.

$$Risk(X_{t,f}) = \sum_i \Pr(E_i) \sum_p \left[\int_{-\infty}^{\infty} Pr(V_p/E_i, X_{t,f}) \times Sev(E_i, V_p) dV_p \right] \tag{3.39}$$

where,

1. $X_{t,f}$: forecast uncertain loading condition at time t.

2. $Pr(V_p/E_i, X_{t,f})$: probability of the stressed voltage of p^{th} bus for i^{th} contingency and forecast uncertain loading condition.

3. $Pr(E_i)$: probability of i^{th} contingency.

4. $Sev(E_i, V_p)$: Severity function which quantify the impact of the i^{th} contingency

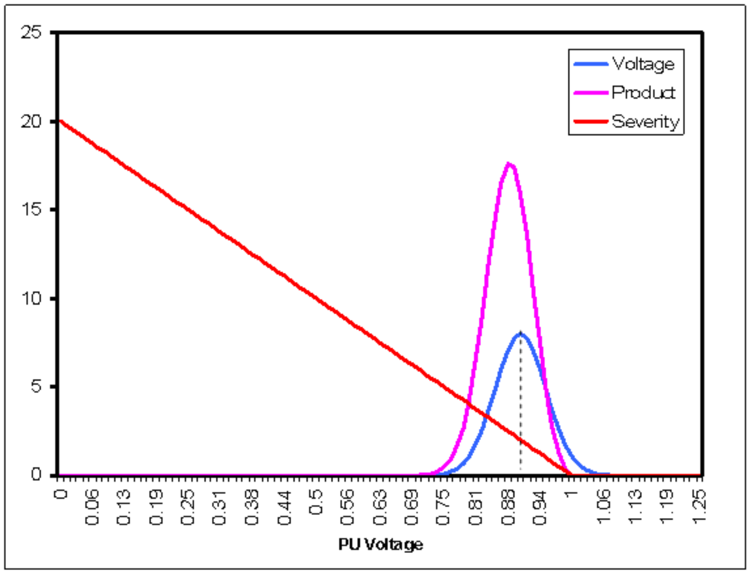

Figure 3.7: Risk Calculation

with variation of the bus voltage.

The IEEE 39 bus test system has been used to demonstrate the risk calculation procedure. A three phase to ground fault is created on the line near the bus bar, and line is removed to clear the fault. After clearing the fault, bus voltages are checked to see whether steady state post disturbance conditions violate any voltage limits. The Newton Raphson power flow is used to calculate the power flow and required sensitivities. Two contingencies are considered, and the first is a three phase to ground fault near the bus 16 on line 16-24 and the second is a three phase to ground fault near the bus 26 on line 26-27. Each fault was cleared after 8 cycles by isolating the faulted line from the system. The continuous severity function is used to calculate the risk index for each contingency. The calculated risk indices for the contingency 1 and the contingency 2 are shown in Table 3.1. The voltage risk indices are graphically shown in Figure 3.8 and 3.9.

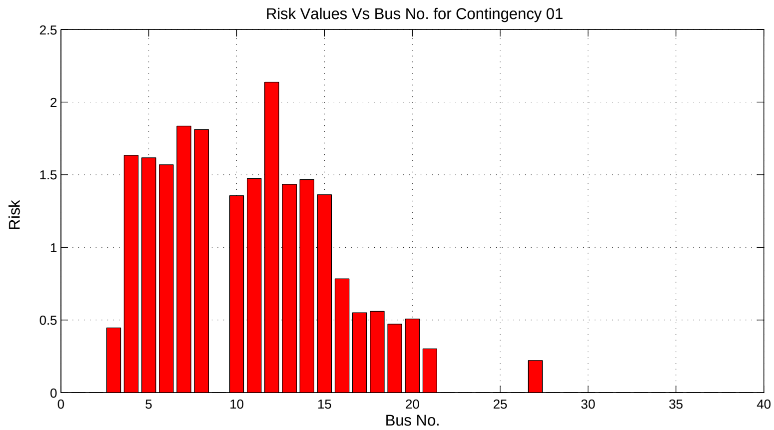

Figure 3.8: Voltage Risk Indices for Contingency 01.

Table 3.1: Voltage Risk for Contingency 1 and 2

Bus Number	**Contingency 01**	**Contingency 02**
3	0.4461	0.7305
4	1.6339	1.7559
5	1.6172	1.6838
6	1.5691	1.6269
7	1.8351	1.8914
8	1.8117	1.8675
10	1.3563	1.4068
11	1.4745	1.5265
12	2.1378	2.1949
13	1.4344	1.4943
14	1.4670	1.5448
15	1.3625	1.4072
16	0.7842	0.8202
17	0.5501	0.9940
18	0.5603	0.9423
19	0.4717	0.4839
20	0.5072	0.5142
21	0.3020	0.4622
24	0.0000	0.5064
27	0.2211	1.5322
Total	**21.5421**	**25.3859**

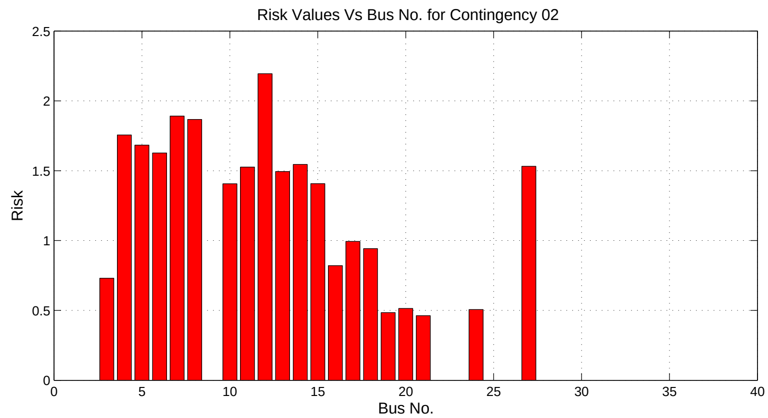

Figure 3.9: Voltage Risk Indices for Contingency 02.

3.4 Risk Based Overload Security Assessment - Linearized Method

In this section, the risk indices for line overloading due to the uncertain P and Q of load buses are calculated. For this calculation, the uncertainty of line flow needed. This uncertainty can be represented as the probability distribution of the line flow. It is assumed that the uncertain load P and Q are normally distributed with base case mean value and known standard deviation. The same procedure as in low voltage risk calculation is used to find the sensitivities of required V and δ with respect to the load P and Q from the Newton Rapson Jacobian matrix. For the line flow sensitivity calculation, the following additional steps need to be considered. If the overloaded line is the line ij then, the sensitivity column matrix can be obtained for line ij with respect to active power P_m as in Equation (3.40) by using matrix manipulation techniques as described in Section 3.3.1. The same sensitivity column matrix need to be obtained for the line ij for all load P and Q.

$$[S_{lij}] = \begin{bmatrix} \frac{\partial \delta_i}{\partial P_m} \\ \frac{\partial \delta_j}{\partial P_m} \\ \frac{\partial V_i}{\partial P_m} \\ \frac{\partial V_j}{\partial P_m} \end{bmatrix} \tag{3.40}$$

From Equations (3.26) to (3.29), the line flow sensitivities with respect to V and δ of i and j buses is obtained as in Equation (3.41).

$$[L_{lij}] = \begin{bmatrix} \frac{\partial P_{ij}}{\partial \delta_i} \\ \frac{\partial P_{ij}}{\partial \delta_j} \\ \frac{\partial P_{ij}}{\partial V_i} \\ \frac{\partial P_{ij}}{\partial V_j} \end{bmatrix} \tag{3.41}$$

By using Equations (3.40) and (3.41), line flow sensitivity with respect to active power load P_m is obtained as in Equation (3.42).

$$\frac{\partial P_{ij}}{\partial P_m} = \begin{bmatrix} \frac{\partial P_{ij}}{\partial \delta_i} & \frac{\partial P_{ij}}{\partial \delta_j} & \frac{\partial P_{ij}}{\partial V_i} & \frac{\partial P_{ij}}{\partial V_j} \end{bmatrix} \times \begin{bmatrix} \frac{\partial \delta_i}{\partial P_m} \\ \frac{\partial \delta_j}{\partial P_m} \\ \frac{\partial V_i}{\partial P_m} \\ \frac{\partial V_j}{\partial P_m} \end{bmatrix} \tag{3.42}$$

By using the same procedure, line flow sensitivity matrix with respect to all load P and Q can be obtained. The resultant sensitivity matrix is presented in Equation (3.43) where nL is the number of load buses in the power system.

$$[S_p] = \left[\begin{array}{c} \frac{\partial P_{ij}}{\partial P_1} \\ \vdots \\ \frac{\partial P_{ij}}{\partial P_{nL}} \\ \hline \frac{\partial P_{ij}}{\partial Q_1} \\ \vdots \\ \frac{\partial P_{ij}}{\partial Q_{nL}} \end{array}\right] \tag{3.43}$$

By using the variance-covariance matrix previously defined in Equation (3.33) and line flow sensitivities in Equation (3.43), the variance of the line flow ij due to the uncertainty of the load P and Q is obtained as in Equation (3.44).

$$\gamma_{P_{ij}} = \left[\begin{array}{cccccc} \frac{\partial P_{ij}}{\partial P_1} & \ldots & \frac{\partial P_{ij}}{\partial P_{nL}} & \frac{\partial P_{ij}}{\partial Q_1} & \ldots & \frac{\partial P_{ij}}{\partial Q_{nL}} \end{array}\right] \times \left[\begin{array}{cccc} \sigma^2_{P_1} \ldots & 0 & 0 \ldots & 0 \\ \vdots & & & \\ 0 \ldots & \sigma^2_{P_{nL}} & 0 \ldots & 0 \\ 0 \ldots & 0 & \sigma^2_{Q_1} \ldots & 0 \\ \vdots & & & \\ 0 \ldots & 0 & 0 \ldots & \sigma^2_{Q_{nL}} \end{array}\right] \times \left[\begin{array}{c} \frac{\partial P_{ij}}{\partial P_1} \\ \vdots \\ \frac{\partial P_{ij}}{\partial P_{nL}} \\ \frac{\partial P_{ij}}{\partial Q_1} \\ \vdots \\ \frac{\partial P_{ij}}{\partial Q_{nL}} \end{array}\right] \tag{3.44}$$

The standard deviation can be written as,

$$\sigma_{P_{ij}} = \sqrt{\gamma_{P_{ij}}} \tag{3.45}$$

According to the initial assumption, P_{ij} is normally distributed. Therefore, probability distribution of P_{ij} can be written as in Equation (3.46),

$$Pr(P_{ij}) = \frac{1}{\sigma_{P_{ij}}\sqrt{2\pi}}\, e^{-\frac{(P_{ij}-\mu_{P_{ij}})^2}{2\sigma^2_{P_{ij}}}} \tag{3.46}$$

The ratings of the lines are different to each other. Therefore, to get good understanding about the line overloading as well as the ability to use generalized severity function, the percentage of rating is used in risk calculation purposes. To have normalized probability distribution, both mean and standard deviation values should be divided by rating of the line before further calculations. The mean value of the percentage of rating is given in Equation (3.47).

$$PR_{ij} = \frac{\mu_{P_{ij}}}{P_{ij_{rated}}} \tag{3.47}$$

The standard deviation of percentage of rating is given in Equation (3.48).

$$\sigma_{PR_{ij}} = \frac{\sigma_{P_{ij}}}{P_{ij_{rated}}} \tag{3.48}$$

Therefore, new probability distribution of the percentage of rating is given in Equation (3.49).

$$Pr(PR_{ij}) = \frac{1}{\sigma_{PR_{ij}}\sqrt{2\pi}}\, e^{-\frac{(PR_{ij}-\mu_{PR_{ij}})^2}{2\sigma^2_{PR_{ij}}}} \tag{3.49}$$

The Risk indices are calculated for the contingency 01 where the fault occurred on line 16-24 and fault is cleared by isolating the faulted line. The risk based static security index is calculated for each and every overloaded line for the P and Q load deviation of 2% as shown in Figure 3.10 and 3.11. The risk indices are given in Table 3.2.

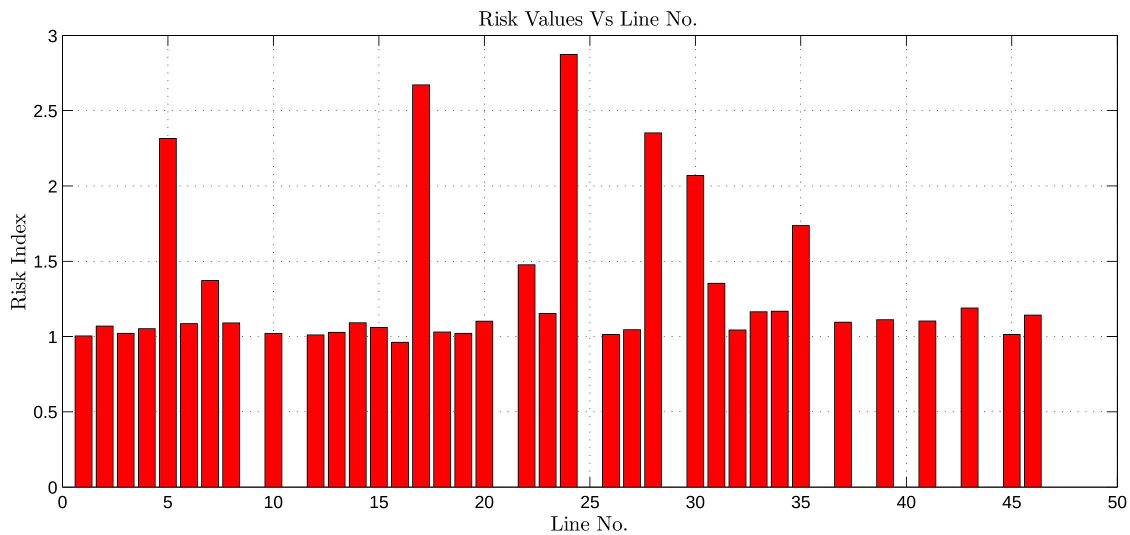

Figure 3.10: Line Flow Risk Indices for Contingency 01.

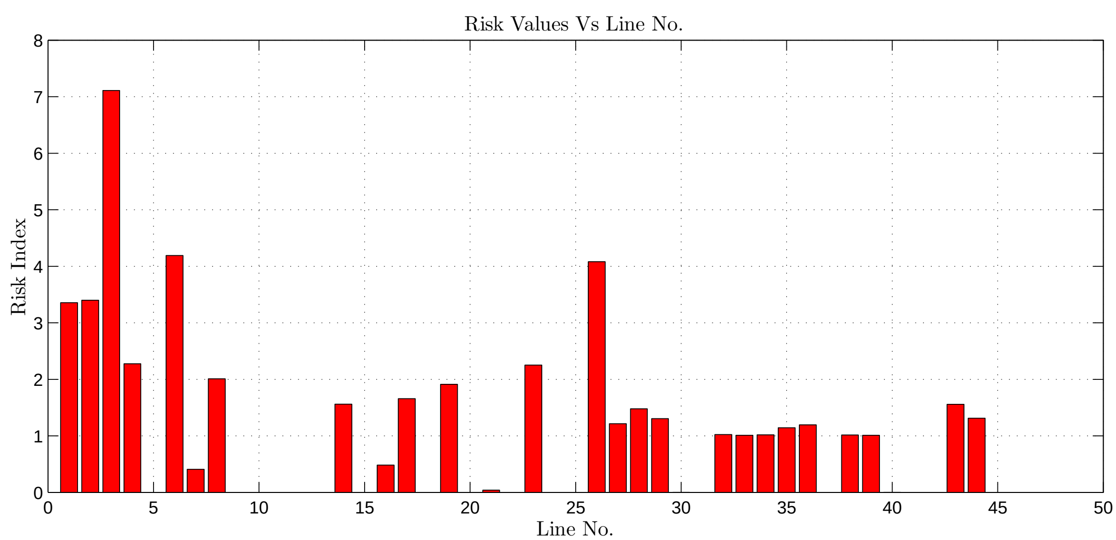

Figure 3.11: Line Flow Risk Indices for Contingency 02.

Table 3.2: Line Flow Risk Indices for Contingency 1 and 2.

Line Number	**Contingency 01**	**Contingency 02**
1	1.0038	3.3563
2	1.0697	3.3994
3	1.0209	7.1113
4	1.0519	2.2751
5	2.3156	0.0000
6	1.0856	4.1906
7	1.3715	0.4073
8	1.0901	2.0084
10	1.0203	0.0000
12	1.0104	0.0000
13	1.0278	0.0000
14	1.0912	1.5621
15	1.0605	0.0000
16	0.9621	0.4836
17	2.6716	1.6589
18	1.0295	0.0000
19	1.0210	1.9125
20	1.1017	0.0000
21	0.0000	0.0388
22	1.4760	0.0000
23	1.1526	2.2513
24	2.8733	0.0000
26	1.0135	4.0803
27	1.0449	1.2161
28	2.3525	1.4793
29	0.0000	1.3041
30	2.0695	0.0000
31	1.3538	0.0000
32	1.0429	1.0232
33	1.1639	1.0113
34	1.1683	1.0175
35	1.7363	1.1423
36	0.0000	1.1948
37	1.0953	0.0000
38	0.0000	1.0146
39	1.1113	1.0105
40	0.0000	0.0004
41	1.1031	0.0000
43	1.1897	1.5592
44	0.0000	1.3117
45	1.0136	0.0000
46	1.1426	0.0000
Total	**47.1082**	**49.0209**

3.5 Validation against the Non-Linear model using Monte Carlo Simulation

In this simulation, the P and Q of the load buses are randomly varied assuming the distributions of these variables are normal with known standard deviations and mean values to incorporate the uncertain operating conditions. In the linear approximated method in Section 3.3 and 3.4, same uncertain load condition have been implemented using linear approximated techniques and sensitivities to find the probability distribution of voltages and line flows. The following random number generation model is used to generate normally distributed P and Q loads. For the k^{th} pre-contingent operating point, the active and reactive power of the i^{th} load bus is given in Equations (3.50) and (3.51).

$$P_L^i(k) = P_{LO}^i\{1 + \varepsilon_{PL}^i(k) * \sigma_P\} \tag{3.50}$$

$$Q_L^i(k) = Q_{LO}^i\{1 + \varepsilon_{QL}^i(k) * \sigma_Q\} \tag{3.51}$$

where,

1. P_{LO}^i,Q_{LO}^i : base case load real and reactive power at the i^{th} bus.

2. $\varepsilon_{PL}^i(k), \varepsilon_{QL}^i(k)$: normally distributed random variable with zero mean and unity standard deviation.

3. σ_P, σ_Q : standard deviation of normally distributed real and reactive power.

By using the Equations (3.50) and (3.51), P and Q of the load buses are randomly varied over normally distribution with known mean and standard deviation. The mean load values are same as base case forecast load values. For each of the randomly generated power system operating points, power flow is solved and the corresponding V and δ are recorded. This process is continued up to 10,000 new cases. The probability distribution of voltages are obtained from generated histogram, and mean and standard deviation of normal distributions are recorded. In the case of line flow, the calculated V and δ values are used to find the power flow through the lines, and the probability distribution of line flows are also recorded from the generated histogram. In this thesis, the distribution of stressed bus voltages and line flows are obtained for two contingencies and for the load standard deviations of 1%, 2%, 5% and 10% cases using generated histogram. These two contingencies are used to demonstrate the linear method and validation against the non-linear method.

3.5.1 Comparison of Linear and Non Linear results

The voltage risk indices calculated using linear method and non-linear method are presented in Figure 3.12 and 3.13 for 2% load standard deviation for contingency 01 and 02.

It can be seen in Figure (3.12) and (3.13) the risk indices calculated form linear method and non-linear methods are approximately equal. The Table (3.3) and (3.4) compare the Risk indices calculated from both linear and non-linear method for contingency 01 and 02.

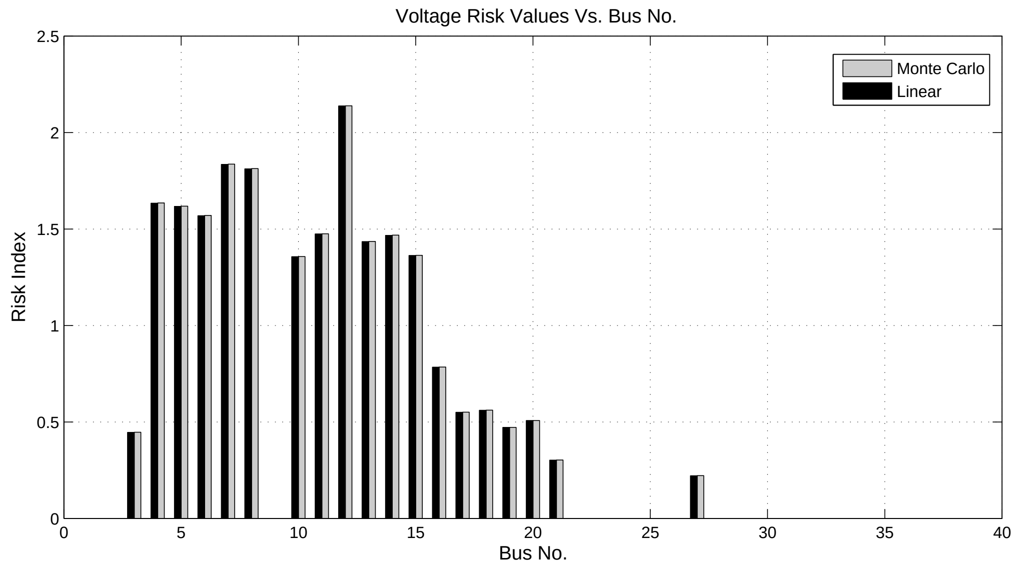

Figure 3.12: Voltage Risk from Non-Linear and Linear methods for contingency 01.

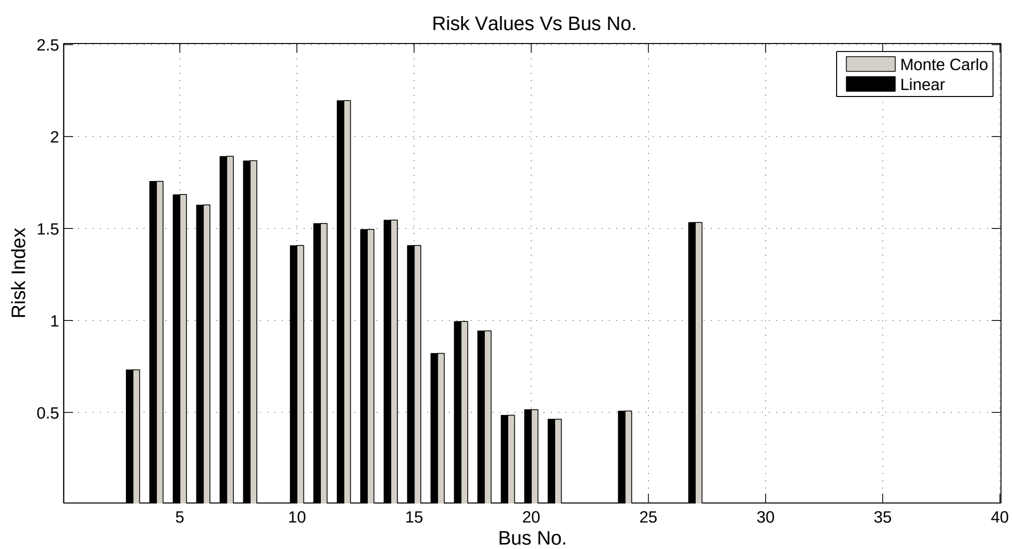

Figure 3.13: Voltage Risk from Non-linear and Linear methods contingency 02.

Table 3.3: Voltage risk from Non-linear and Linear methods for contingency 01.

Bus No.	For 2 % load σ		
	Non-linear	Linear	Error %
3	0.4468	0.4461	-0.17
4	1.6350	1.6339	-0.07
5	1.6185	1.6172	-0.08
6	1.5703	1.5691	-0.08
7	1.8363	1.8351	-0.07
8	1.8130	1.8117	-0.07
10	1.3572	1.3563	-0.07
11	1.4755	1.4745	-0.07
12	2.1388	2.1378	-0.05
13	1.4354	1.4344	-0.07
14	1.4680	1.4670	-0.07
15	1.3634	1.3625	-0.06
16	0.7849	0.7842	-0.09
17	0.5508	0.5501	-0.13
18	0.5610	0.5603	-0.13
19	0.4721	0.4717	-0.07
20	0.5074	0.5072	-0.04
21	0.3025	0.3020	-0.18
27	0.2217	0.2211	-0.25

3.6 Concluding Remarks

In risk based static security assessment, the risk indices calculated from both linear and non-linear methods are almost equal to each other. Therefore, linear method is validated from non-linear method. The Monte Carlo simulation method is a time consuming method as large number of cases have to be run to get the probability distribution of performance measures such as bus voltages and branch flows. Therefore, in practical control room environment, the Monte Carlo method can not be used. Although linear method uses first order partial derivatives for index calculation, it indicates accurate results for small load deviations which is adequate to incorporate one-hour ahead load forecast uncertainty. However, for large load deviations the first

Table 3.4: Voltage risk from Non-linear and Linear methods for contingency 02.

Bus No.	For 2 % load σ		
	Non-linear	Linear	Error %
3	0.7313	0.7305	-0.12
4	1.7571	1.7559	-0.07
5	1.6852	1.6838	-0.08
6	1.6283	1.6269	-0.09
7	1.8929	1.8914	-0.08
8	1.8691	1.8675	-0.08
10	1.4078	1.4068	-0.07
11	1.5276	1.5265	-0.07
12	2.1961	2.1949	-0.05
13	1.4954	1.4943	-0.07
14	1.5459	1.5448	-0.07
15	1.4082	1.4072	-0.07
16	0.8210	0.8202	-0.09
17	0.9949	0.9940	-0.09
18	0.9432	0.9423	-0.10
19	0.4842	0.4839	-0.07
20	0.5143	0.5142	-0.03
21	0.4627	0.4622	-0.12
24	0.5071	0.5064	-0.14
27	1.5333	1.5322	-0.07

order approximation of partial derivatives are not accurate, and the calculated indices deviate from each other between linear and non-linear methods.

Chapter 4

Risk Based Dynamic Security Assessment

4.1 Introduction

Dynamic security assessment determines whether the power system reaches a new equilibrium operating point after the transition. Most of the dynamic security assessment studies have been done in deterministic way in the past as mentioned in Chapter 2. Although, simple probabilistic approaches of the dynamic security assessment is rare in the literature, time consuming Monte Carlo simulation methods have been extensively used. The availability of transient stability margin in functional form [9] and risk based static security approaches [8, 10] make it possible to carry out probabilistic dynamic security assessment using linear approaches. These linear methods are accurate for small load deviations, and they are adequate to model the one-hour ahead load forecast uncertainty. Therefore, it can be used in control room environment with available computing power and it allows to take operation decisions within a short time period. The calculation time of the dynamic risk index is presented in

Section 5.2 using a standard personal computer.

Chapter 3 discussed the probabilistic static security assessment both in linear and non-linear methods. In this Chapter, same methods are extended for dynamic security assessment and validated using Monte Carlo simulation.

4.2 Transient Stability Margin in Functional form

The transient stability margin in functional form have been derived in [9] with respect to V and δ and details of derivation and the application of this model into IEEE 39 bus teat system have been explained.

The operating point of the power system can be uniquely defined by identifying $2n - 1$ specific operating parameters, where n is the number of generator and load buses of the power system [6]. There are different types of power system variables that can be selected to represent the power system. However, most effective and convenient way is to select the generator and load bus voltages and angles.

The transient stability of the power system is described as the ability of the power system to maintain synchronism when subjected to a severe transient disturbances such as a fault on transmission facilities, loss of generation, or loss of a large load [6]. The boundary between transiently stable and unstable regions can be identified with respect to above identified operating parameters. In the past, nomograms have been used to identify the stable and unstable regions [29]. The method used in nomograms is a two-dimensional simple approach to distinguish stable and unstable region of the power system. However, with the availability of high speed computing power [30], more advanced multi dimensional techniques have been developed.

In this thesis, the functional form of the transient stability boundary generated from machine learning techniques have been used to calculate the risk based dynamic security index. It has been shown in [9] that multi dimensional functional form of transient stability boundary can be generated using techniques known as Kernel Ridge Regression. The off line generated database is used to form and train as well as to check the accuracy of the generated function.

The generated polynomial can be used to estimate the critical clearing time of the power system for a particular contingency. The derived function given in Equation (4.1) is a polynomial of m^{th} order and was generated from data samples of n_t training points.

$$f(x) \approx \sum_{i=1}^{n_t} \alpha_i(< x, x_i > +1)^m \tag{4.1}$$

Where, α=[α_1,.....α_{n_t}] is a vector of scalar parameters and n_t is the number of samples in the training set and m is the degree of nonlinearity of the polynomial.

The database was generated using a commercially available transient stability assessment program and a total of 1365 data points were generated. From the generated data, 955 points were used to estimate the polynomial and remaining 410 points were used to test the accuracy of the polynomial. An accuracy of 95% was observed for the IEEE 39 bus test system.

The generated polynomial is differentiable with respect to specific operating parameters and required sensitivities are obtained with respect to V and δ of all the buses for the risk calculation.

The first order partial derivative of the polynomial with respect to j^{th} power flow variables is given in Equation (4.2).

$$\frac{\partial f(x)}{\partial x_j} \approx \sum_{i=1}^{n} \alpha_i m(< x, x_i > +1)^{m-1} x_{ij} \tag{4.2}$$

The polynomial form of the transient stability margin is derived for two contingencies: first is a three phase to ground fault near the bus 16 on the line 16-24 and second is a three phase to ground fault near the bus 26 on the line 26-27. Both were cleared after 8 cycles by isolating the faulted line from the system. The values of α and m are obtained by using optimization techniques [9] and for contingency 1, $m = 6$ and for contingency 2, $m = 4$.

4.3 Probability Distribution of Stability Margin

4.3.1 Linear Method

To find the probability distribution of stability margin, partial derivatives of the stability margin are obtained from Equation (4.2), and the resultant sensitivities used for risk calculation are shown in Equation (4.3).

$$STV_{SM_i} = \begin{bmatrix} \frac{\partial SM_i}{\partial \delta_1} & \dots & \frac{\partial SM_i}{\partial \delta_n}, & \frac{\partial SM_i}{\partial |V_1|} & \dots & \frac{\partial SM_i}{\partial |V_n|} \end{bmatrix} \tag{4.3}$$

As described in Chapter 3, the partial derivatives of the V and δ can be obtained with respect to load bus P and Q by inverting the Newton Raphson Jacobian matrix . For a Power system with hundreds of buses, direct inversion is difficult and therefore, partial derivatives of all load bus P and Q with respect to V and δ as in Equation (4.4) can be obtained from manipulation of standard load flow Jacobian matrix. If the requirement is to calculate the sensitivity of the stability margin for contingency k and for the active power P of i^{th} load bus, then the required column vector of the inverse Jacobian matrix is given in Equation (4.4).

$$[S_J] = \begin{bmatrix} \frac{\partial \delta_1}{\partial P_i} \\ \vdots \\ \frac{\partial \delta_n}{\partial P_i} \\ \frac{\partial |V_1|}{\partial P_i} \\ \vdots \\ \frac{\partial |V_n|}{\partial P_i} \end{bmatrix} \tag{4.4}$$

The required matrix for all the sensitivity calculation is shown in Equation (4.5), where nL is the number of load buses and n is the total number of buses in the system.

$$[S_a] = \left[\begin{array}{ccc|ccc} \frac{\partial \delta_1}{\partial P_1} & \cdots & \frac{\partial \delta_1}{\partial P_{nL}} & \frac{\partial \delta_1}{\partial Q_1} & \cdots & \frac{\partial \delta_1}{\partial Q_{nL}} \\ \vdots & & & & & \\ \frac{\partial \delta_n}{\partial P_1} & \cdots & \frac{\partial \delta_n}{\partial P_{nL}} & \frac{\partial \delta_n}{\partial Q_1} & \cdots & \frac{\partial \delta_n}{\partial Q_{nL}} \\ \hline \frac{\partial |V_1|}{\partial P_1} & \cdots & \frac{\partial |V_1|}{\partial P_{nL}} & \frac{\partial |V_1|}{\partial Q_1} & \cdots & \frac{\partial |V_1|}{\partial Q_{nL}} \\ \vdots & & & & & \\ \frac{\partial |V_n|}{\partial P_1} & \cdots & \frac{\partial |V_n|}{\partial P_{nL}} & \frac{\partial |V_n|}{\partial Q_1} & \cdots & \frac{\partial |V_n|}{\partial Q_{nL}} \end{array}\right] \tag{4.5}$$

Then by using Equations (4.3) and (4.4), the sensitivity of the stability margin with respect to active power P of the i^{th} load bus can be calculated as in Equation (4.6) for the k^{th} contingency.

$$\frac{\partial SM_k}{\partial P_i} = \begin{bmatrix} \frac{\partial SM_i}{\partial \delta_1} & \dots & \frac{\partial SM_i}{\partial \delta_n} & \frac{\partial SM_i}{\partial |V_1|} & \dots & \frac{\partial SM_i}{\partial |V_n|} \end{bmatrix} \times \begin{bmatrix} \frac{\partial \delta_1}{\partial P_i} \\ \vdots \\ \frac{\partial \delta_n}{\partial P_i} \\ \\ \frac{\partial |V_1|}{\partial P_i} \\ \vdots \\ \frac{\partial |V_n|}{\partial P_i} \end{bmatrix} \tag{4.6}$$

Above calculation is continued for each and every load bus and partial derivatives of stability margin with respect to all load bus P and Q are obtained as shown in Equation (4.7).

$$[S_p] = \begin{bmatrix} \frac{\partial SM_k}{\partial P_1} \\ \vdots \\ \frac{\partial SM_k}{\partial P_{nL}} \\ \hline \frac{\partial SM_k}{\partial Q_1} \\ \vdots \\ \frac{\partial SM_k}{\partial Q_{nL}} \end{bmatrix} \tag{4.7}$$

The same variance-covariance matrix in Equation (3.33), which was used in Chapter 3 can be used to calculate the variance of the stability margin as in Equation (4.8).

$$\gamma_{SM_k} = \begin{bmatrix} \frac{\partial SM_k}{\partial P_1} & \dots & \frac{\partial SM_k}{\partial P_{nL}} & \frac{\partial SM_{ij}}{\partial Q_1} & \dots & \frac{\partial SM_k}{\partial Q_{nL}} \end{bmatrix} \times \begin{bmatrix} \sigma^2_{P_1} \dots & 0 & 0 \dots & 0 \\ \vdots & & & \\ 0 \dots & \sigma^2_{P_{nL}} & 0 \dots & 0 \\ 0 \dots & 0 & \sigma^2_{Q_1} \dots & 0 \\ \vdots & & & \\ 0 \dots & 0 & 0 \dots & \sigma^2_{Q_{nL}} \end{bmatrix} \times \begin{bmatrix} \frac{\partial SM_k}{\partial P_1} \\ \vdots \\ \frac{\partial SM_k}{\partial P_{nL}} \\ \frac{\partial SM_k}{\partial Q_1} \\ \vdots \\ \frac{\partial SM_k}{\partial Q_{nL}} \end{bmatrix} \tag{4.8}$$

Then the standard deviation can be obtained as,

$$\sigma_{SM_k} = \sqrt{\gamma_{SM_k}} \tag{4.9}$$

According to the initial assumption SM_k is normally distributed and therefore, the probability distribution of SM_k is,

$$Pr(SM_k) = \frac{1}{\sigma_{SM_k}\sqrt{2\pi}}\, e^{-\frac{(SM_k - \mu_{SM_k})^2}{2\sigma^2_{SM_k}}} \tag{4.10}$$

The above probability distribution is normalized by using Equations (4.11) and (4.12). The ACT is the Actual fault clearing time of the power system and for the IEEE 39 bus test system it is 8 cycles. For risk index calculation purposes this ACT is used. The mean value of the distribution is given in Equation (4.11).

$$SM_{k_{NORMALIZED}} = \frac{\mu_{SM_k}}{ACT} \tag{4.11}$$

The standard deviation of the stability margin is given in Equation (4.12).

$$\sigma_{SM_{k_{NORMALIZED}}} = \frac{\sigma_{SM_k}}{ACT} \tag{4.12}$$

The procedure of linear approximated method is presented by a flow chart in

Figure (4.1).

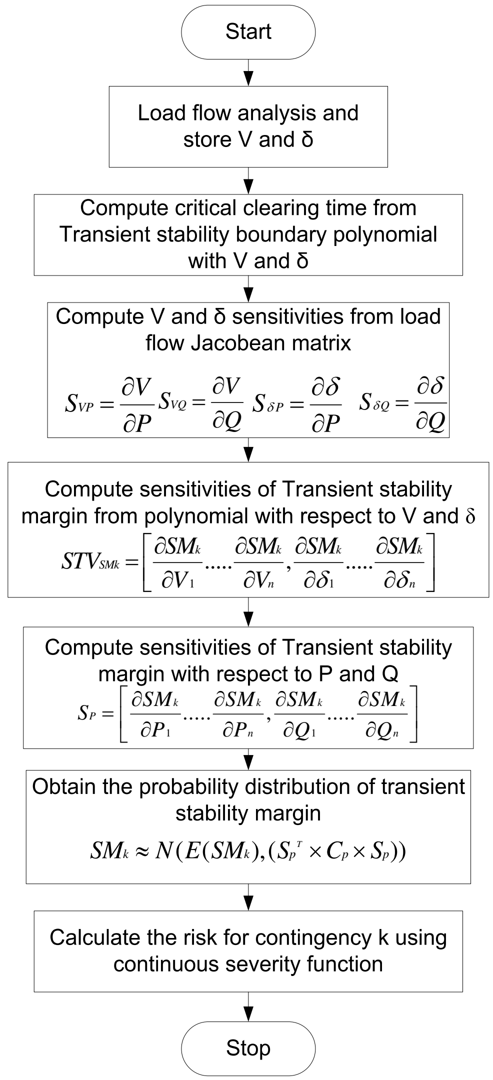

Figure 4.1: Flowchart of Linear approximation method.

4.3.2 Non Liner Model using Monte Carlo Technique

In non-linear method, the P and Q of the load buses are randomly varied over normal distribution with known standard deviations and mean values to implement the uncertain operating conditions. However, in the linear method in Section 4.3.1, same uncertain load condition have been implemented using linear approximated techniques to find the probability distribution of stability margin. The steps of the Monte Carlo simulation based risk calculation are illustrated in Figure 4.3 in a block diagram format. Non-linear method is used to check the accuracy of the proposed linear approach. The mean load values are the same as the base case forecast load values. For each of the randomly generated power system operating point, power flow is solved and the corresponding V and δ of all buses are recorded. For these operating points, the stability margin is determined using the polynomial given in [9] for each contingency. This process is continued up to 10,000 replications and the probability distribution of the transient stability margin is obtained for selected load standard deviations of 1%, 2%, 5% and 10% cases using generated histogram. The probability distribution of transient stability margin for 10,000 replications with 2% load standard deviation for contingency 1 is shown in Figure 4.2. The equivalent normal distribution obtained from the proposed linear method is also included in Figure 4.2 for comparison. It can be seen from Figure 4.2 that the probability distribution obtained from non linear method is virtually identical to the equivalent normal distribution obtained from the proposed linear method for 2% load standard deviation. Therefore, it is clear that when the load standard deviation is small, the assumption of normally distributed stability margin is acceptable.

The probability distribution of stability margin as well as risk indices are compared with both linear approach and non-linear method.

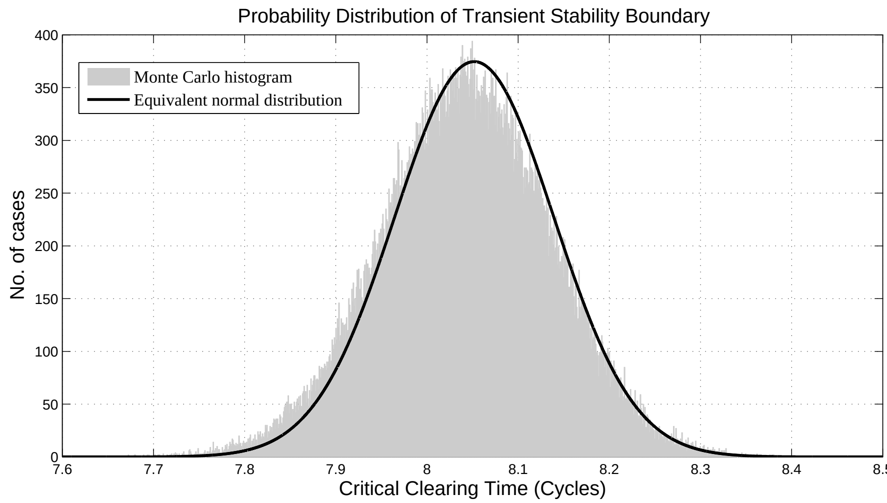

Figure 4.2: Histogram and equivalent normal distribution of Transient Stability Margin for 10,000 cases with 2% load standard deviation for contingency 1.

The probability distribution of transient stability margin for 10,000 replications with 10% load standard deviation for contingency 2 is shown in Figure 4.4. The equivalent normal distribution obtained from the proposed linear method is also included in Figure 4.4 for comparison. Non-linearly generated probability distribution and equivalent normal distribution are not matching as for 2% load standard deviation. Therefore, it is noticed that, when the load standard deviation is high the assumption made for normally distributed transient stability margin is not valid and this leads to higher error percentages.

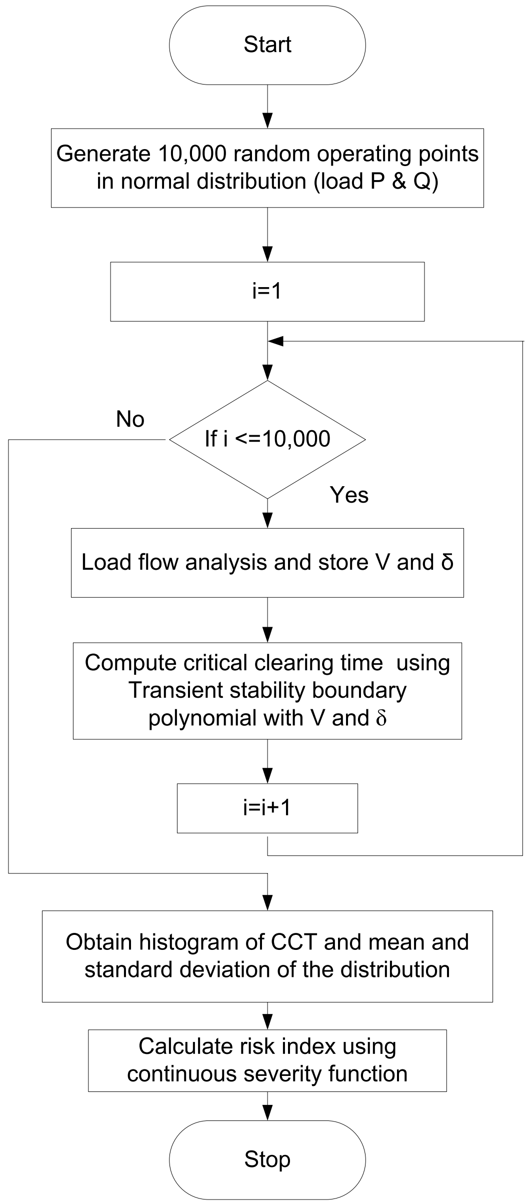

Figure 4.3: Flowchart of Monte Carlo based simulation.

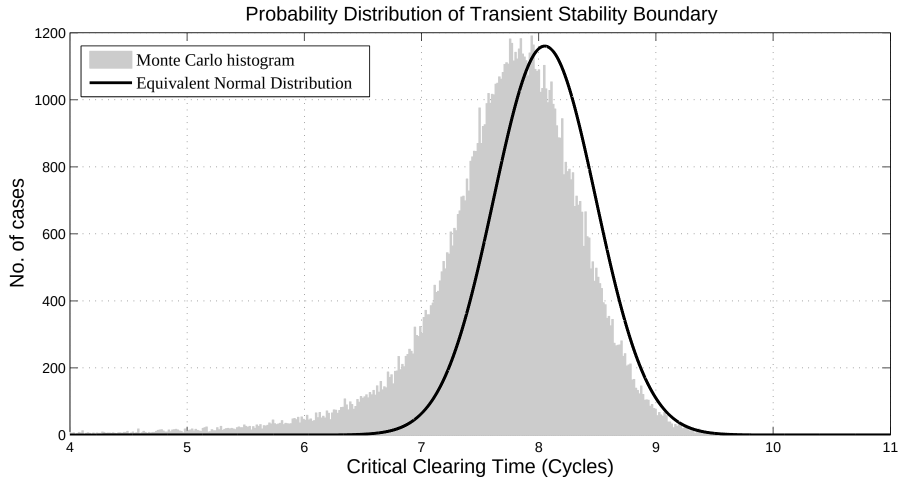

Figure 4.4: Histogram and equivalent normal distribution of Transient Stability Margin for 10,000 cases with 10% load standard deviation for contingency 2.

4.3.3 Comparison of Probability Distributions

The calculated mean values and standard deviations are compared for contingency 01 in Table 4.1 and contingency 02 in Table 4.2 of both linear and non-Linear methods for different load standard deviations. The percentage error is presented for both mean value and standard deviation by taking Monte Carlo generated value as base value. The comparison of error with load standard deviation is illustrated in Figure 4.5 and Figure 4.6 for contingency 01 and 02 respectively.

Table 4.1: Mean, standard deviation and percentage error of Stability Margin by Non Linear and Linear methods for contingency 01.

Load σ	Monte Carlo				Linear	
	Mean	% error	σ	% error	Mean	σ
0.01	8.0928	-0.16	0.02985	-7.12	8.0800	0.02772
0.02	8.0947	-0.18	0.05959	-6.96	8.0800	0.05544
0.05	8.1067	-0.33	0.15019	-7.71	8.0800	0.13861
0.10	8.1463	-0.81	0.31160	-11.03	8.0800	0.27722

Table 4.2: Mean, standard deviation and percentage error of Stability Margin by Non Linear and Linear methods for contingency 02.

Load σ	Monte Carlo				Linear	
	Mean	% error	σ	% error	Mean	σ
0.01	8.0526	-0.01	0.04636	-5.83	8.0518	0.04366
0.02	8.0423	0.12	0.09362	-6.73	8.0518	0.08732
0.05	7.9698	1.03	0.26148	-16.51	8.0518	0.21831
0.10	7.7067	4.48	0.72797	-40.02	8.0518	0.43662

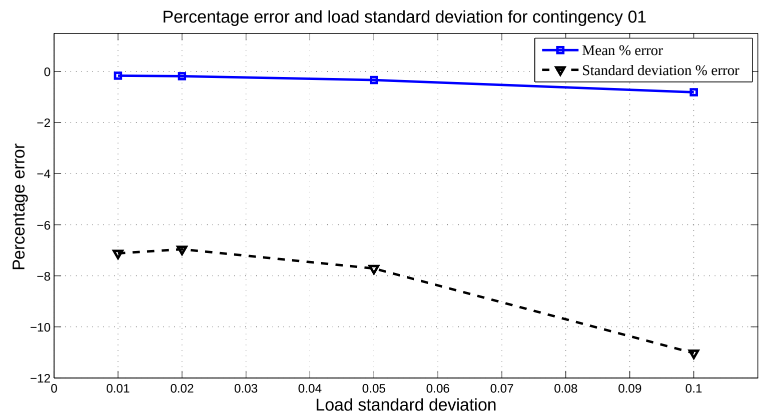

Figure 4.5: Percentage error of mean and standard deviation with load standard deviation for contingency 01.

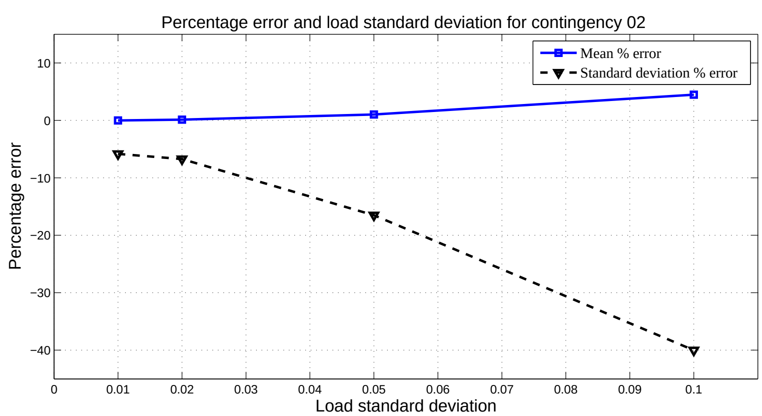

Figure 4.6: Percentage error of mean and standard deviation with load standard deviation for contingency 02.

4.3.4 Risk Calculation

The uncertainty of the stability margin is obtained due to the uncertainty of the load bus P and Q . In the linear method, the continuous severity function model is used to calculate the system risk index for a particular contingency using Equation (4.13). In the dynamic security assessment, the risk index of the power system can be obtained for a particular contingency by single calculation. This is an additional advantage of the dynamic risk index calculation. However, in voltage and line flow risk calculations, all the indices of each voltage and line flow need to be calculated. The risk index for a particular contingency is found by taking the summation of all the indices. In non-linear method, same continuous severity function and probability distribution of stability margin is used to calculate the risk index for each contingency using Equation (4.13). The risk indices calculated using Linear method are validated by non-linear method.

The continuous severity function is presented in Figure 4.7.

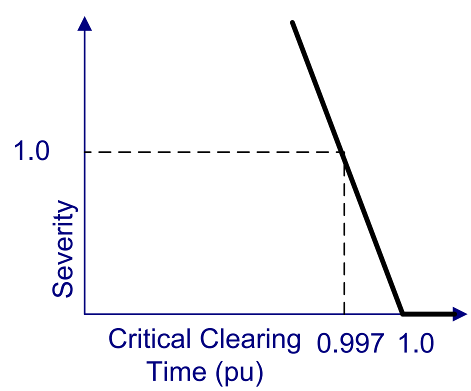

Figure 4.7: Continuous severity function for transient stability margin.

$$Risk(SM_{t,f}) = \sum_i \Pr(E_i) \left[\int_{-\infty}^{\infty} Pr(SM/E_i, X_{t,f}) \times Sev(E_i, SM) dSM \right] \tag{4.13}$$

where,

1. $X_{t,f}$: forecast uncertain loading condition at time t.
2. $Pr(SM/E_i, X_{t,f})$: probability of the stability margin for i^{th} contingency and forecast uncertain loading condition.
3. $Pr(E_i)$: probability of i^{th} contingency.
4. $Sev(E_i, SM)$: severity function which quantify the impact of the i^{th} contingency with variation of stability margin.

The risk indices calculated for both contingencies and for different load deviations are presented in Table (4.3).

Table 4.3: Risk values for two contingencies for different load standard deviation levels.

Load σ	Risk			
	Contingency 01		Contingency 02	
	Non Linear	Linear	Non Linear	Linear
0.01	0.00032	0.00072	0.12390	0.10867
0.02	0.05929	0.07925	0.82120	0.62924
0.05	0.87790	1.01918	5.00400	2.66401
0.10	2.69201	3.14325	19.178000	6.24337

The calculated risk indices are graphically presented in the Figure 4.8 and Figure 4.9 for contingency 01 and contingency 02 respectively.

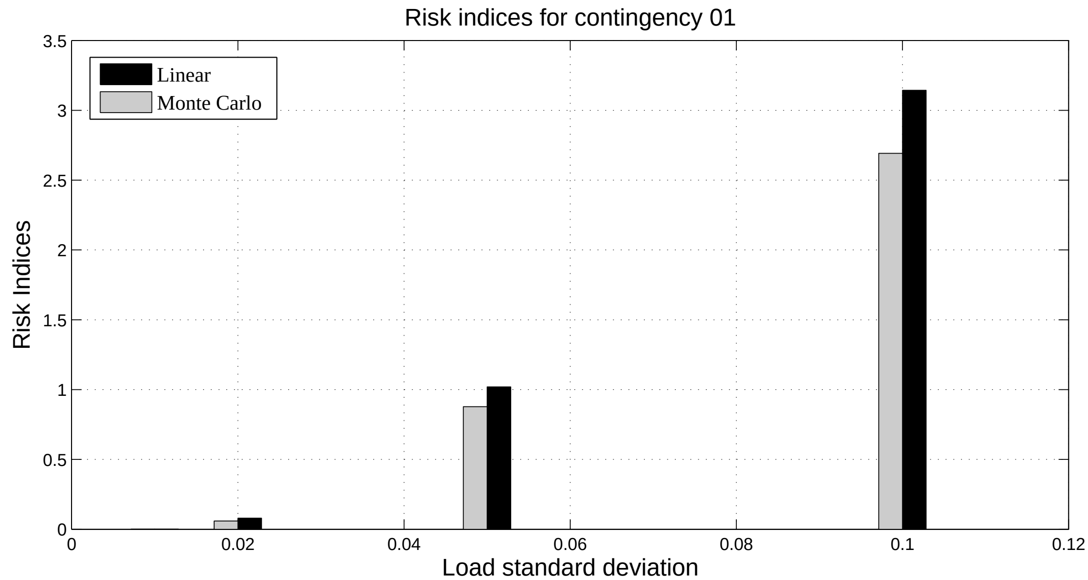

Figure 4.8: Risk comparison for contingency 01.

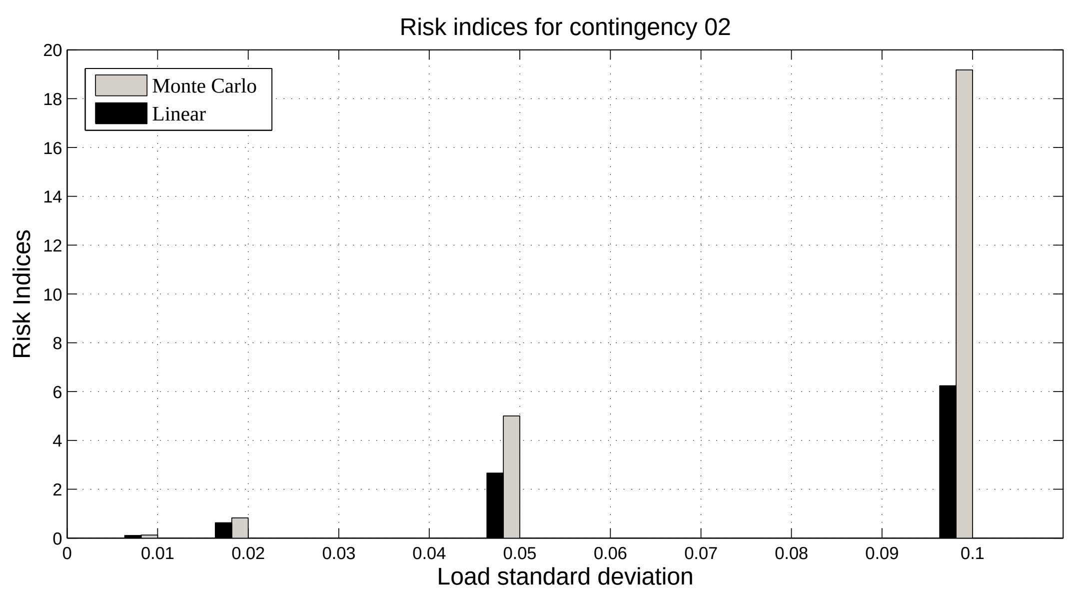

Figure 4.9: Risk comparison for contingency 02.

4.4 Concluding Remarks

In risk based dynamic security assessment, the risk indices calculated from both non-linear and linear methods are approximately equal to each other up to 5% load standard deviations. It is adequate to analyze uncertainty of the one-hour-ahead load forecast. It is noticed that, when the load standard deviation is high the assumption made for normally distributed transient stability margin is not valid and this leads to higher error percentages. The risk values obtained from both methods are very close to each other in contingency 01 as error of mean and standard deviation of the stability margin is low. In contingency 02, risk values are close up to 5% load standard deviation and deviate at 10%. Therefore, linear approximation method is not accurate above 5% load deviations. To check the nonlinearity behavior of the transient stability margin polynomial, second order partial derivatives are calculated. The absolute average value of second order partial derivatives of contingency 02 is 9.42 and for contingency 01 it is 0.75. These results confirmed that contingency 02 is more non linear than contingency 01 at considered power system operating point. Therefore, higher error percentage of probability distributions as well as risk indices can be expected from contingency 02.

As described in the Chapter 3 the Monte Carlo simulation method is time consuming as large number of cases have to be run to get the probability distribution of transient stability margin. Therefore, in practical control room environment the Monte Carlo method can not be used. However, linear method uses first order partial derivatives for risk index calculation and it indicates accurate results for small load deviations. Furthermore, for large load deviations the first order approximation of partial derivatives are not accurate and the calculated indices deviate from each other between linear and non-linear method.

Chapter 5

Applications and Issues

5.1 Introduction

The applications of the risk based dynamic security index at the control room environment is discussed in this Chapter. The operators at the control room can effectively use the dynamic risk index and operate the power system in a secure manner by selecting the lowest risk operating scenarios. The limitations associated with calculation of the transient stability margin in functional form and the dynamic risk index is presented.

5.2 Applications and Issues with One-Hour-Ahead Forecast

According to the results presented in the previous section, the proposed method is computationally very efficient and accurate for small load standard deviations up to 5%. The applicability of this method therefore relies on the fact that the expected load standard deviation is small (5%). If the load forecast used here is a one-hour-ahead forecast, it is reasonable to assume that the deviation from the forecast is within

$\pm$5%. Therefore, the main question is whether, all the necessary computations can be completed with the one-hour time period available. Total time required for one contingency is the sum of the time taken to complete the following tasks.

- Generation of 100 data points around the forecast load and computation of transient stability margin for each data point (t_1=180s).
- Estimation of functional form of transient stability margin (t_2=0.1s).
- Calculation of risk index from proposed linear model (t_3=0.36s).

It has been found that in [9], 100 data points are adequate to estimate the functional form of transient stability margin with more than 95% classification accuracy within (t_1+t_2) s.

All the computations presented in this thesis were carried out using a AMDx2 1.9GHz PC for the IEEE 39 bus test system. Total system risk can be calculated within 180.46n_c s ((t_1+t_2+t_3)$\times n_c$), where n_c is the number of probable contingencies. Therefore, for the IEEE 39 bus test system, approximately 20 contingencies can be handled using 1 computer with one-hour-ahead forecast. Data generation and computation of transient stability margin is the most time intense tasks and parallel processing can be used for higher number of contingencies.

5.3 Applications at the Control Room

Suppose there are only two probable contingencies available in the IEEE 39 bus test system. Assume that the probability of the contingency 1 and contingency 2 is 0.05 and 0.03 respectively within the next hour. If the load forecast uncertainty of the next hour is 5%, then from Table 4.3, individual risk components for the given operating conditions are 1.01918 and 2.66401 for contingency 1 and contingency 2. Therefore, total dynamic risk of the power system can be calculated using Equation 4.13.

$$Risk(SM_{t,f}) = (0.05 \times 1.01918) + (0.03 \times 2.66401) = 0.1308793 \qquad (5.1)$$

Assume that, the threshold value of 0.12 is set for the total dynamic risk considering the past experience and analysis at the control room. The operating conditions should be adjusted to lower the total dynamic risk below 0.12 by the control room operator. These operating conditions could be generation levels, power flow levels or voltage levels. If risk is higher than the threshold level (0.12), then the operation of the IEEE 39 bus power system is not secure.

Chapter 6

Conclusions

6.1 General Conclusions

The linearized method for calculating risk based dynamic security index has been presented in this thesis. The calculated risk index has been validated by developing Monte Carlo type simulation. The proposed linearized method has been used to calculate the risk based dynamic security index of two contingencies for IEEE 39 bus test system.

The results have shown a good correlation of two approaches with low load standard deviation levels. This is adequate to analyze the effect of uncertainty of the one-hour-ahead load forecast on dynamic security of the power systems. Therefore, this validated teh accuracy of the linear approximation method and it can be used to calculate the total system risk with less computing resources as well as within short period of time. As a result of highly competitive uncertain electricity market, stressed conditions arises more often than before and identification of risky operating conditions is much important to prevent total system failures as well as to take corrective actions to prevent them. Therefore, these risk indices can be used as a guideline to check the danger of different operating conditions to take preventive action before failure happens.

Total system risk is obtained by calculating the individual risk components of normal contingency set and weighting these risk components according to the probability of each contingency. The iso risk contours can be drawn in two dimensional plot by changing the power system operating points and compared with deterministic dynamic security limits.

The concept of risk based security assessment has been introduced in Chapter 2, and the way this method could be developed for risk based dynamic security assessment has been presented.

The risk based static security assessment of the power system was presented in Chapter 3, and risk indices for low voltage and line overload have been calculated for two contingencies. The risk based static security models developed in the literature have been validated using Monte Carlo simulation.

In Chapter 4, the risk based dynamic security assessment model has been developed by extending the risk based static security assessment models and polynomial form of transient stability boundary. The calculated dynamic risk indices have been validated using Monte Carlo simulation.

The applications and issues of the proposed risk bases dynamic security index have been presented in Chapter 5.

For a particular power system, threshold value of the risk index need to be identified to compare different operating points with all higher probable contingencies. The operation of the power system is not acceptable beyond threshold level. The proposed indices can be used as a guideline for control room security related economic decision making as high stressed operating conditions arise more frequently in competitive market environment. For this, economical modeling of severity function is required and it should represent economic impact of contingencies.

The proposed method can be applied for larger power systems to calculate the total risk based dynamic security index with all higher probable contingencies.

6.2 Contributions

The main contributions of the work presented in this thesis are as follows.

- Validated the accuracy of the linearized risk based static security assessment models using Monte Carlo simulation for low voltage and line overload.
- Developed a power system load data generation model to implement Monte Carlo simulation.
- Developed a linearized risk based dynamic security assessment model for transient stability and validated using Monte Carlo simulation.

6.3 Suggestions for Future Research

The work presented in this thesis has developed basic foundation for risk based dynamic security assessment by using polynomial form of transient stability boundary. The following work can be carried out to enhance the usage of risk based dynamic security assessment model.

- The risk index calculation has been limited to two contingencies as the derivation of the transient stability polynomial is much time consuming. Therefore, risk index can be generated for selected contingency set, which has the highest probability and impact on the power system. Finally total dynamic risk of the power system can be calculated.

- The developed method can be applied to the larger power systems and risk indices can be calculated.

- The equal risk contours can be drawn with different generation and load flow levels and that can be compared with deterministic security contours.

- The continuous severity function has been used for risk index calculation. Furthermore, the realistic severity functional model can be developed to represent the actual impact of the contingency by including economic aspect of the contingency.

- The assumed variance-covariance matrix has been used here to represent the uncertainty of operating conditions. The actual variance-covariance matrix can be developed by collecting actual data from the power system. This should represent the true behavior of the power system.

Appendix A

Test Systems Data

A.1 New England 39 Bus System

A.1.1 Single Line Diagram

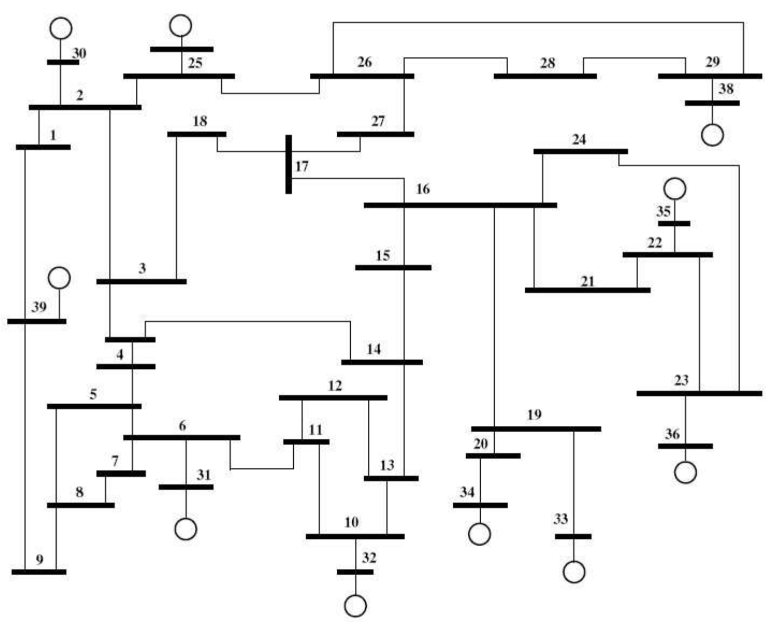

Figure A.1: Single Line Diagram of IEEE New England 39 Bus System.

A.1.2 Power Flow - AC Bus Data

Bus				Voltage	
Number	Name	Base kV	Type	Magnitude	Angle
1	LOAD 1 500.	500	Load Bus	1.0369	-9.5558
2	LOAD 2 500.	500	Load Bus	1.0219	-6.5211
3	LOAD 3 500.	500	Load Bus	0.9959	-9.1261
4	LOAD 4 500.	500	Load Bus	0.9607	-9.9175
5	LOAD 5 500.	500	Load Bus	0.9585	-8.8347
6	LOAD 6 500.	500	Load Bus	0.9594	-8.1001
7	LOAD 7 500.	500	Load Bus	0.9518	-10.4807
8	LOAD 8 500.	500	Load Bus	0.9524	-11.0584
9	LOAD 9 500.	500	Load Bus	1.0102	-11.2726
10	LOAD 10 500.	500	Load Bus	0.9658	-5.4844
11	LOAD 11 500.	500	Load Bus	0.9624	-6.3757
12	LOAD 12 500.	500	Load Bus	0.9441	-6.3440
13	LOAD 13 500.	500	Load Bus	0.9646	-6.2007
14	LOAD 14 500.	500	Load Bus	0.9662	-7.8587
15	LOAD 15 500.	500	Load Bus	0.9752	-7.9415
16	LOAD 16 500.	500	Load Bus	0.9931	-6.4120
17	LOAD 17 500.	500	Load Bus	0.9974	-7.6697
18	LOAD 18 500.	500	Load Bus	0.9956	-8.6507
19	LOAD 19 500.	500	Load Bus	0.9922	-0.9434
20	LOAD 20 500.	500	Load Bus	0.9892	-1.8371
21	LOAD 21 500.	500	Load Bus	0.9999	-3.9461
22	LOAD 22 500.	500	Load Bus	1.0245	0.5102
23	LOAD 23 500.	500	Load Bus	1.0236	0.3068
24	LOAD 24 500.	500	Load Bus	1.0010	-6.2540
25	LOAD 25 500.	500	Load Bus	1.0302	-5.1310
26	LOAD 26 500.	500	Load Bus	1.0220	-6.2040
27	LOAD 27 500.	500	Load Bus	1.0053	-8.0106
28	LOAD 28 500.	500	Load Bus	1.0225	-2.8474
29	LOAD 29 500.	500	Load Bus	1.0231	-0.1119
30	GEN 30 500	500	Gen. Bus	1.0475	-4.3227
31	GEN 31 500	500	Swing Bus	0.9820	0.0000
32	GEN 32 500	500	Gen. Bus	0.9831	1.9201
33	GEN 33 500	500	Gen. Bus	0.9972	3.9352
34	GEN 34 500	500	Gen. Bus	1.0123	3.0839
35	GEN 35 500	500	Gen. Bus	1.0493	5.2212
36	GEN 36 500	500	Gen. Bus	1.0635	7.8266
37	GEN 37 500	500	Gen. Bus	1.0278	1.2660
38	GEN 38 500	500	Gen. Bus	1.0265	6.5945
39	GEN 39 500	500	Gen. Bus	1.0300	-11.3128

A.1.3 Power Flow - Load Data

Bus Number	MW	MVAr
3	307.43	2.29
4	465.50	171.30
7	218.78	78.60
8	513.75	173.22
12	7.18	84.27
15	292.75	139.97
16	316.93	31.11
18	146.35	27.79
20	593.02	97.26
21	256.66	107.72
23	226.43	77.40
24	282.91	-84.52
25	214.72	45.24
26	136.41	16.68
27	259.74	69.79
28	199.03	26.67
29	276.87	26.27
31	8.40	4.20
39	1062.43	240.59

A.1.4 Power Flow - Generator Data

Bus Number	MW	MVAr
30	226.86	152.74
31	539.14	130.47
32	611.84	124.47
33	594.10	31.11
34	483.53	126.22
35	617.40	207.60
36	527.09	180.75
37	508.63	4.49
38	787.63	28.00
39	930.95	197.93

A.1.5 Power Flow - Line Data

From Bus	To Bus	Series		Charging	
Number	Number	Resistance	Reactance	Conductance	Susceptance
1	2	0.00350	0.04110	0.00000	0.69870
1	39	0.00100	0.02500	0.00000	0.75000
2	3	0.00130	0.01510	0.00000	0.25720
2	25	0.00700	0.00860	0.00000	0.14600
2	30	0.00000	0.01810	0.00000	0.00000
3	4	0.00130	0.02130	0.00000	0.22140
3	18	0.00110	0.01330	0.00000	0.21380
4	5	0.00080	0.01280	0.00000	0.13420
4	14	0.00080	0.01290	0.00000	0.13820
5	6	0.00020	0.00260	0.00000	0.04340
5	8	0.00080	0.01120	0.00000	0.14760
6	7	0.00060	0.00920	0.00000	0.11300
6	11	0.00070	0.00820	0.00000	0.13890
6	31	0.00000	0.02500	0.00000	0.00000
7	8	0.00040	0.00460	0.00000	0.07800
8	9	0.00230	0.03630	0.00000	0.38040
9	39	0.00100	0.02500	0.00000	1.20000
10	11	0.00040	0.00430	0.00000	0.07290
10	13	0.00040	0.00430	0.00000	0.07290
10	32	0.00000	0.02000	0.00000	0.00000
11	12	0.00160	0.04350	0.00000	0.00000
12	13	0.00160	0.04350	0.00000	0.00000
13	14	0.00090	0.01010	0.00000	0.17230
14	15	0.00180	0.02170	0.00000	0.36600
15	16	0.00090	0.00940	0.00000	0.17100
16	17	0.00070	0.00890	0.00000	0.13420
16	19	0.00160	0.01950	0.00000	0.30400
16	21	0.00080	0.01350	0.00000	0.25480
16	24	0.00030	0.00590	0.00000	0.06800
17	18	0.00070	0.00820	0.00000	0.13190
17	27	0.00130	0.01730	0.00000	0.32160
19	20	0.00070	0.01380	0.00000	0.00000
19	23	0.00070	0.01420	0.00000	0.00000
20	34	0.00090	0.01800	0.00000	0.00000
21	22	0.00080	0.01400	0.00000	0.25650
22	23	0.00060	0.00960	0.00000	0.18460
23	24	0.00220	0.03500	0.00000	0.36100
25	26	0.00320	0.03230	0.00000	0.51300
25	37	0.00060	0.02320	0.00000	0.00000
26	27	0.00140	0.01470	0.00000	0.23960
26	28	0.00430	0.04740	0.00000	0.78020
26	29	0.00570	0.06250	0.00000	1.02900
28	29	0.00140	0.01510	0.00000	0.24900
29	38	0.00080	0.01560	0.00000	0.00000

Per unit values are based on 100MVA rating.

A.1.6 Dynamic Data - Generators

IBUS	T'do	T"do	T'qo	T"qo	H	D	Xd	Xq	X'd	X'q	X"d	Xl	MVA	Rsource
30	10.20	0.05	1.50	0.06	4.20	0.400	1.00	0.69	0.31	0.30	0.30	0.125	1000	0.000
31	6.56	0.05	1.50	0.06	3.03	0.975	2.95	2.82	0.70	1.67	0.60	0.350	1000	0.000
32	5.70	0.05	1.50	0.06	3.58	1.000	2.50	2.37	0.53	0.88	0.50	0.304	1000	0.000
33	5.69	0.05	1.50	0.06	2.86	1.000	2.62	2.58	0.44	1.43	0.40	0.295	1000	0.000
34	5.40	0.05	0.44	0.06	2.60	0.300	6.70	6.20	1.32	1.66	1.30	0.540	1000	0.000
35	7.30	0.05	0.40	0.06	3.48	1.000	2.54	2.41	0.50	0.81	0.40	0.224	1000	0.000
36	5.66	0.05	1.50	0.06	2.64	0.800	2.95	2.92	0.50	1.67	0.50	0.322	1000	0.000
37	6.70	0.05	0.41	0.06	2.43	0.900	2.90	2.80	0.57	0.91	0.50	0.280	1000	0.000
38	4.79	0.05	1.96	0.06	3.45	1.400	2.11	2.05	0.57	0.70	0.50	0.298	1000	0.000
39	7.00	0.05	1.50	0.06	50.00	1.000	0.20	0.19	0.06	0.51	0.05	0.030	1200	0.000

A.1.7 Dynamic Data - Exciters (IEEET1)

Bus Number	TR	KA	TA	KE	TE	KF	TF
30	0.001	5.0	0.06	1.00	0.250	0.040	1.00
31	0.001	6.2	0.05	0.06	0.405	0.057	0.50
32	0.001	5.0	0.06	1.00	0.500	0.080	1.00
33	0.001	5.0	0.06	1.00	0.500	0.080	1.00
34	0.001	20.0	0.02	1.00	0.785	0.030	1.00
35	0.001	5.0	0.02	1.00	0.471	0.075	1.25
36	0.001	40.0	0.02	1.00	0.730	0.030	1.00
37	0.001	5.0	0.02	1.00	0.528	0.085	1.26
38	0.001	40.0	0.02	1.00	1.400	0.030	1.00
39	0.001	40.0	0.02	1.00	1.400	0.030	1.00

A.1.8 Dynamic Data - Stabilizer (STAB1)

Bus Number	K/T	T	T1/T3	T3	T2/T4	T4
30	14.0	0.05	6.1	0.04	6.1	0.04
31	6.0	0.05	5.5	0.07	5.5	0.07
32	17.0	0.05	5.8	0.04	5.8	0.04
33	2.5	0.05	3.7	0.10	3.7	0.10
34	15.0	0.05	3.5	0.07	3.5	0.07
35	8.0	0.05	4.2	0.05	4.2	0.05
37	2.5	0.05	7.8	0.04	7.8	0.04
38	15.0	0.05	4.5	0.07	4.5	0.07
39	38.0	0.05	5.0	0.09	5.0	0.09

Acronyms

CCT	Critical Clearing Time
CIGRE	International Council on Large Electric Systems
DSA	Dynamic Security Assesment
IEEE	Institution of Electrical and Electronics Engineers
SM	Stability Margin
TSB	Transient Stability Boundary
RBSSI	Risk Based Static Security Index
RBDSI	Risk Based Dynamic Security Index

References

[1] IEEE Working Group Report (M.B.Guertin), "Reliabilty indices for use in bulk power system supply adequacy evaluation", *IEEE Transactions on Power Apparatus and Systems*, vol. PAS-97, no. 4, pp. 1097–1103, July/Aug 1978.

[2] CIGRE TF 38.03.12 Report (R.J.Marceau and J.Endrenyi), "Power System Security Assessment:A Position Paper", *ELECTRA*, , no. 175, pp. 48–78, December 1997.

[3] Prabha Kundur, John Paserba, Venkat Ajjarapu, Goran Andersson, Anjan Bose, Claudio Canizares, Nikos Hatziargyriou, David Hill, Alex Stankovic, Carson Taylor, Thierry Van Cutsem, and Vijay Vittal, "Definition and classification of power system stability", *IEEE Transactions on Power Systems*, vol. 19, no. 2, pp. 1387–1401, May 2004.

[4] Byung Ha Lee and Kwang Y. Lee, "Dynamic and Static Voltage Stability Enhancement of Power Systems", *IEEE Transactions on Power Systems*, vol. 8, no. 1, pp. 231–238, February 1993.

[5] G. K. Morison, B. Gao, and P. Kundur, "Voltage Stability Analysis Using Static and Dynamic Approoaces", *IEEE Transactions on Power Systems*, vol. 8, no. 3, pp. 1159–1171, August 1993.

[6] P. Kundur, *Power System Stability and Control*, McGrew-Hill, Inc, 1994.

[7] Lester H. Fink and Kjell Carlsen, "Operating Under Stress and Strain", IEEE spectrum, March 1978, vol. 15, pp. 48–53.

[8] Ming Ni, James D. McCalley, Vijay Vittal, and Tayyib Tayyib, "Online Risk-Based Security Assesment", *IEEE Transactions on Power Delivery*, vol. 18, no. 1, pp. 258–265, February 2003.

[9] Bathiya Jayasekara and Udaya D. Annakkage, "Derivation of an Accurate Polynomial Representation of the Transient Stability Boundry", *IEEE Transactions on Power Delivery*, vol. 21, no. 4, pp. 1856–1863, November 2006.

[10] James D. McCalley, Vijay Vittal, and Nicholas Abi-Samra, "An Overview of Risk Based Security Assessment", Proceedings of the IEEE Power Engineering Society Summer Power Meeting, July 1999, vol. 1, pp. 173–178.

[11] J. McCalley, S. Asgarpoor L.Bertling, R.Billinton, H. Chao, J. Chen, J. Endrenyi, R. Fletcher, C. Grigg, G. Hamoud, D. Logan, A. P. Meliopoulos, M. Ni, N. Rau, L. Salvaderi, M. Schilling, Y. Schlumberger, A. Schneider, and C. Singh, "Probabilistic Security Assessment for Power System Operations", Proceedings of the IEEE Summer Meeting, Denver, CO., June 2004, vol. 1, pp. 212–220.

[12] R. Billinton and P. R. S. Kuruganty, "A Probabilistic Index for Transient Stability", *IEEE Transactions on Power Apparatus and Systems*, vol. PAS-99, no. 1, pp. 195–206, Jan/Feb 1980.

[13] P. R. S. Kuruganty and R. Billinton, "Protection System Modeling in a Probabilistic Assessment of Transient Stability", *IEEE Transactions on Power Apparatus and Systems*, vol. PAS-100, no. 5, pp. 2163–2170, May 1981.

[14] R. Billinton and P.R.S. Kuruganthy, "Probabilistic Assessment of Transient Stability in a Practical Multimachine System", *IEEE Transactions on Power Apparatus and Systems*, vol. PAS-100, no. 7, pp. 3634–3642, July 1981.

[15] R. Billinton and S. Aboreshaid, "Stochastic Modeling of High-Speed Reclosing in Probabilistic Transient Stability Studies", *IEEE Proceedings on Power Systems*, vol. 142, no. 4, pp. 350–354, July 1995.

[16] Saleh Aboreshaid, Roy Billinton, and Mahmud Fotuhi-Firuzabad, "Probabilistic Trnasient Stability Studies Using the Method of Bisection", *IEEE Transactions on Power Systems*, vol. 11, no. 4, pp. 1990–1995, November 1996.

[17] Saleh Aboreshaid and Roy Billinton, "A Framework for Incorporating Voltage and Transient Stability Consideration in Well-Being Evalauation of Composite Power Systems", *Proceedings of the IEEE Power Engineering Society Summer Power Meeting*, vol. 1, pp. 219–224, July 1999.

[18] Ebrahim Vaahedi, Wenyuan Li, Timothy Chia, and Hermann Dommel, "Large Scale Probabilistic Transient Stability Assessment Using B.C. Hydro Online Tool", *IEEE Transactions on Power Delivery*, vol. 15, no. 2, pp. 661–667, May 2000.

[19] Wenyuan Li, *Risk Assesment of Power Systems, Models, Methods and Applications*, IEEE Press series on power engineering,A John Wiley & Sons, Inc., 2005.

[20] Ming Ni, James D. McCalley, Vijay Vittal, Scott Greene, Chee-Wooi Ten, Vijaya Sudhakar Ganugula, and Tayyib Tayyib, "Software Inplimenation of Online Risk-Based Security Assesment", *IEEE Transactions on Power Delivery*, vol. 18, no. 3, pp. 1165–1172, August 2003.

[21] Hua Wan, James D. McCalley, and Vijay Vittal, "Risk Based Voltage Security Assesment", *IEEE Transactions on Power Systems*, vol. 15, no. 4, pp. 1247–1254, November 2000.

[22] Fei Xiao and James D. MacCalley, "Power System Risk Assessment and Control in a Multiobjective Framework", *IEEE Transactions on Power Systems*, vol. 24, no. 1, pp. 78–85, February 2009.

[23] Neal Balu, Timothy Bertram, Anjin Bose, Vladimir Brandwajn, Gerry Cauley, David Curtice, Aziz Fouad, Lester Fink, Mark G. Lauby, Bruce F. Wollenberg, and Joseph N. Wrubel, "Online Power System Security Analysis", *IEEE Transactions on Power Delivery*, vol. 80, no. 2, pp. 262–282, February 1992.

[24] James D. McCalley, A. A. Fouad, Baj L. Agrawal, and Richard G. Farmer, "A Risk-Based Security Index for Determinig Operating Limits in Stability-Limited Electric Power Systems", *IEEE Transactions on Power Delivery*, vol. 12, no. 3, pp. 1210–1219, August 1997.

[25] Weihui Fu and James D. McCalley, "Risk Based Optimal Power Flow", Power Tech Proceedings, 2001 IEEE Porto, September 2001, vol. 3.

[26] M. A. Pai, *Energy Function Analysis for Power System Stability*, Kluwer Academic Publishers, 1989.

[27] Hadi Saadat, *Power System Analysis*, McGrew-Hill, Inc, 2002.

[28] A report prepared by the Reliability Test System Task Force of the Application of Probability Methods Subcommittee, "The IEEE Reliability Test System-1996", *IEEE Transactions on Power Systems*, vol. 14, no. 3, pp. 1010–1020, August 1999.

[29] Study Committee 38 CIGRE TF-38.02.17, Task Force 17, "Advance Angle Stability Controls", December 1999.

[30] L. S. Moulin, A. P. A. da Silva, M. A. El-Sharkawi, and R. J. Marks, "Support vector machines for transient stability analysis of large-scale power systems", *IEEE Transactions on Power Apparatus and Systems*, vol. 19, no. 2, pp. 818825, May 2004.